UNIVERSIDAD MICHOACANA
DE SAN NICOLÁS DE HIDALGO

Faculty of Chemical Engineering

PhD in Chemical Engineering

Optimal design of ocean thermal energy conversion systems

PHD THESIS

To obtain the Degree of Doctor in Chemical Engineering

Presents:

M.C.I.Q Ilse María Hernández Romero

DISSERTATION

Submitted in partial fulfillment of the requirements for the degree of Doctor of Chemical Engineering in the Graduate College of the Universidad Michoacana de San Nicolas de Hidalgo

- Advisor: Dr. Fabricio Nápoles Rivera
- Co-Advisor: Dr. Luis Fabián Fuentes Cortés

Morelia, Michoacán; August 2021

ACKNOWLEDGEMENT

To Dr. Fabricio Nápoles Rivera and Dr. Luis Fabián Fuentes Cortés for their advice during my training as a researcher, for their advice and shared knowledge. Thank you for your constant support and for the opportunity to collaborate with you.

To Dr. Victor M. Zavala (UW-Madison) and Dr. Antonio Flores Tlacuahuac (ITESM) for their hospitality in their Institutions, for guiding me in new perspectives within the process area and the vision in the generation and writing of scientific articles.

To Dr. José María Ponce Ortega, Dr. Rafael Huirache Acuña and Dr. Luis Fernando Lira, for their reviews, points of view as experts in their respective areas of research and contributions made at each stage of the project.

To Brenda González: not only for opening the doors of your house to me, but also for the incredible friendship that took place, thank you for the good conversations that contributed to the transformation of my thinking in many social aspects thanks to your experience and knowledge in the area.

To my friends Nayra and Chechi for their unconditional friendship and support in each of my decisions.

To my friend Land for her unconditional friendship, for her collaboration and support in the development of my thesis and for sharing many moments with me.

To my friends Alex Cadena, Heri, Lili and Felipe, for all the shared moments, the stay abroad thanks to you was like being at home.

To my friends Juan Martínez and Ramón Gonzales for their friendship, company and support during all this time. Also, for their collaboration as researchers.

To colleagues in the systems optimization group at UW – Madison Joshua P, Hani Yoo, Yicheng Hu, Apoorva Sampat and Renkee Kuhlmann for their support, patience and the things I learned, both professionally and personally.

To the Faculty of Chemical Engineering and the Mexican Council Science and Technology (CONACyT) for all the economic and administrative support during this project.

DEDICATION

I dedicate my dissertation work to my family and many friends. A special feeling of gratitude to my parents, Lazaro and Edith whose words of encouragement and push for tenacity ring in my ears. To my sisters Vera, Kary, Dahian and Pao for all your support and love. To my nephew Gadi and my niece Verita for all their love. To my brother in law Eli, my grandparents Hermi y Cirilo, my aunt Mary and my dear cousins Sil and Citla for all their unconditional support. To all of them, my family who are my driving force and my inspiration to be and give the best of myself.

I also dedicate my work to my friends Nayra, Chechi, Land, Leydi, Brenda G., Alex C., Heriberto A., Lili, Felipe, Paulina Baker, Mary Knoche, Elizabeth G, Juan M, Ramón G. Hany Y, Jesse, Yolis, Lina, Juan P. Thank you for your support, for being there to talk, share a drink, a good conversation and a good time.

"One never notices what has been done; one can only see what remains to be done"
Marie Curie

TABLE OF CONTENTS

List of Figures

List of Tables

Nomenclature

Acronyms	
Cw	*cold seawater*
cw,o	*cold seawater out flowrate from the condenser*
cw,in	*cold seawater taken from the ocean*
2	*compressed liquid*
Con	*condenser*
Ev	*evaporator*
G	*generator*
4	*liquid-vapor mixture*
M	*motor of the pump*
OTEC	*ocean thermal energy conversion*
3	*overheated vapor*
Pp	*piping*
P	*pumps*
1	*saturated liquid*
Sw	*seawater*
SWAC	*Seawater air-conditioning system*
Sc	*solar collector*
sc,o	*solar collector output*
Tr	*turbine*
ws	*warm seawater*
ws,o	*warm seawater out flowrate from the evaporator*
ws,in	*warm seawater taken from the ocean*
Wf	*working fluid*
Sets	
t={1,2,3...24}	*time (hours)*
s={1,2,3...4}	*seasons of the year (Spring, Summer, Fall, Winter)*

n={1,2,3...N}	*components of the cycle (Tr, G, M, sc, p, pp,ev, con)*
Variables	
A	*area,* m^2
CCCOST	*capital cost,$*
CS	*compromise solution*
H	*enthalpy, kWh/kg*
S	*entropy, kJ/kg° K*
$\dot{E}x$	*exergy balance*
$\psi^{exergetic}$	*exergetic efficiency*
Q	*heat transferred, kWh*
MCOST	*maintenance cost ,$*
m	*mass, kg*
ΔTml	*mean logarithmic temperature, °C*
η^{cycle}	*net cycle efficiency*
OCOST	*operational cost,$*
P	*pressure, MPa*
$\eta_{t,s}^{sc}$	*solar collector efficiency*
T	*temperature, °C*
TAC	*total annual cost, $*
W	*working, kWh*
Parameters	
κ_1	*1st order heat loss coefficient,* W/m^2 *°C*
κ_2	*2nd order heat loss coefficient,* W/m^2 $°C^2$
η	*efficiency*
k_F	*factor used to annualize the capital costs,* y^{-1}
FC	*fixed cost, $*
g	*gravity,* m/s^2
H_Y	*hours of operation, h*

U	*overall heat transfer coefficient, kW/m^2 °C*
η_0	*optical efficiency*
D	*pipeline diameter*
L	*pipeline length*
km, v	*pipe cost parameters that depend on the pipe material*
PPC	*pumping cost*
δ	*scaling factor*
Cp^{sw}	*seawater calorific capacity, kWh/Kg°C*
$Eg_{t,s}$	*solar irradiance, kWh/m^2*
To, ho, So	*temperature, enthalpy and entropy as a ambient conditions*
UC	*unitary cost, $*
U^{ma}	*unitary cost per maintenance, $*
VC	*wariable cost, $*
$T_s^{ws,in}$	*warm seawater temperature seasonal variation, °C*

Abstract

"Optimal design of ocean thermal energy conversion systems

Ilse María Hernández Romero, August 2021

Currently, there is a worldwide problem due to the increase in energy demands, which in the turn brings with it negative effects on the environment due to the consumption of non-renewable resources and the use of fossil fuels for electricity generation to the daily emission of large amounts of greenhouse gases into the atmosphere. Concern about the threat of global climate change points to the investigation of alternative sources of renewable energy for the supply of energy from different sources. The ocean represents 70% of the planet's surface, which can be considered an inexhaustible source of renewable energy. This makes it the largest collector and storage system for solar energy. This is the origin of ocean thermal energy conversion (OTEC) systems, systems that work by taking advantage of the naturally occurring temperature differential between the warm surface layers and the cold deep seawater to generate electricity. Therefore, this work proposes the study and optimization of OTEC power cycles to generate electricity considering technical, economic, environmental and social aspects. However, the design and control of these systems involves multiple factors associated with the treatment of energy demand, environmental conditions, technology design, energy market costs and environmental impact. The generated models allow determining the technological configuration and sizing of the system, as well as the operation policy. The results show how to trade-off system design and operation with conflicting objective functions.

Keywords: Ocean thermal energy conversion systems, Multi-objective optimization, closed power cycle, Renewable energy, Desalinated water

Resumen

"Diseño óptimo de sistemas de conversión de energía térmica oceánica"

Ilse María Hernández Romero, Agosto 2021

Actualmente se tiene una problemática mundial por el incremento en las demandas energéticas que a su vez traen consigo efectos negativos en el medio ambiente por el consumo de los recursos no renovables y el uso de combustibles fósiles para la generación de energía eléctrica, además de que diariamente emiten grandes cantidades de gases de efecto invernadero a la atmósfera. La preocupación por la amenaza del cambio climático mundial apunta a la investigación de fuentes alternas de energía renovable para el suministro de energía de diferentes fuentes. El océano representa el 70% de la superficie del planeta, los cuales pueden ser considerados como una fuente inagotable de energía renovable. Esto lo hace el colector más grande y sistema de almacenamiento de energía solar. De aquí surgen los sistemas de conversión de energía térmica oceánica (OTEC), sistemas que funcionan aprovechando el diferencial de temperatura que ocurre de manera natural entre las capas superficial caliente y el agua de mar profunda fría para generar electricidad. Por lo tanto, en este trabajo se propone el estudio y optimización de los ciclos de potencia OTEC para generar electricidad considerando aspectos técnicos, económicos, ambientales y sociales. Sin embargo, el diseño y control de estos sistemas envuelve múltiples factores asociados con el tratamiento de la demanda energética, condiciones ambientales, el diseño de las tecnologías, los costos del mercado energético y el impacto ambiental. Los modelos generados permiten determinar la configuración tecnológica y el dimensionamiento del sistema, así como la política de operación. Los resultados muestran como compensar el diseño y operación del sistema con funciones objetivo en conflicto.

Palabras clave: Sistemas de energía térmica oceánica, Optimización multi-objetivo, Ciclo cerrado de potencia, Energía renovable, Agua desalinizada.

1. Introduction

Increasing energy demands, coupled with the threat of climate change, present a suitable scenario for developing renewable energy and energy efficiency techniques, as well as improving existing ones. There are factors that point to investment in sustainable energy: The constant volatility of oil prices, dependence on other countries, and the big amounts of greenhouse gas emissions from energy consumption resulting from energy transformation. The growing use of fossil fuels, associated with the increase in population and the increase in living standards in general, brings with it the production of greenhouse gas emissions, so the use of renewable energies such as: solar, wind, hydraulic, oceanic, etc., aim to be a key factor for the production of sustainable energy in the future. In this way, the exponential growth of the world population has led to significant increases in energy consumption coupled with the generation of greenhouse gas emissions (Bakirtas & Akpolat, 2018). In Mexico, around 80% of power generation is performed using fossil fuels like coal, natural gas and fuel oil for feeding large-scale plants that operate in a centralized schema. (SENER, 2017). As an effort for reducing environmental impact and stimulating the development of energy transitions, the legal framework was modified recently for stimulating the development of new technologies based on renewable energy sources (Pérez-Denicia et al., 2015). Therefore, Mexico has improved its energy infrastructure during the last years. A significant amount of clean energy is produced using solar photovoltaic systems (Mundo-Hernández et al., 2014), hydroelectric plants, wind farms (Hernández-Escobedo et al. 2018), geothermal (Hiriart & Gutiérrez-Negrín, 2003) and biomass resources (Tauro, 2019). All of them together represent 20 % of the national energy produced (SENER, 2017). Compared with the conditions in near countries, this development could be considered as incipient. In addition, implementation of traditional renewable technologies, as wind farms and photovoltaic systems has produced competitions and conflicts, associated to land usage, involving local rural producers and indigenous communities (Pischke et al., 2019; Zarate-Toledo et al., 2019).

Therefore, it is essential developing and innovate other options for power generation and improving existing technologies in order to satisfy national electricity demand while minimizing the environmental, energetic and social impact (Zhang et al. 2019). In this

context, considering land usage conflicts and need for developing new technologies, the ocean energy represents a sustainable alternative that can be explored (Esteban & Leary, 2012). Systems based on ocean energy as the Ocean Thermal Energy Conversion (OTEC) systems have enormous develop potential considering extensions of coastal areas and the energy used for touristic, harbor activities, fisheries and other coastal activities. This technology can be used for stimulating the implementation of distributed generation units using renewable resources (Rau & Baird, 2018; Fard & Tedeschi, 2018).

OTEC is a system using the temperature difference between the warm surface seawater and cold deep seawater of the ocean to produce thermal energy and connected with a generator is capable to produce electricity (Khan, 2017)(see **Fig. 1**). However, in order to obtain the highest possible efficiency, the thermal gradient between the surface and the deep waters should be at least 20 ˚C. That is, the greater the temperature gradient, the greater the efficiency (Devis-Morales et al., 2014). This technology uses the principles of the Rankine cycle to generate electricity through steam turbines. In this context, different OTEC plant designs are identified according to the working fluid used for electricity generation. The main designs correspond to closed, open and hybrid power cycles. The closed cycle uses a working fluid with a low boiling point and only produces electrical energy, open cycle uses the warm seawater as the working fluid and the hybrid cycle combines both mentioned cycles, the last two can produce electricity and desalinated water as well as secondary products (Kim et al., 2016). Regardless of the type of design of the OTEC cycle, it is necessary to use a working fluid that will allow the thermal gradient to be used for energy production (Yang, 2014).

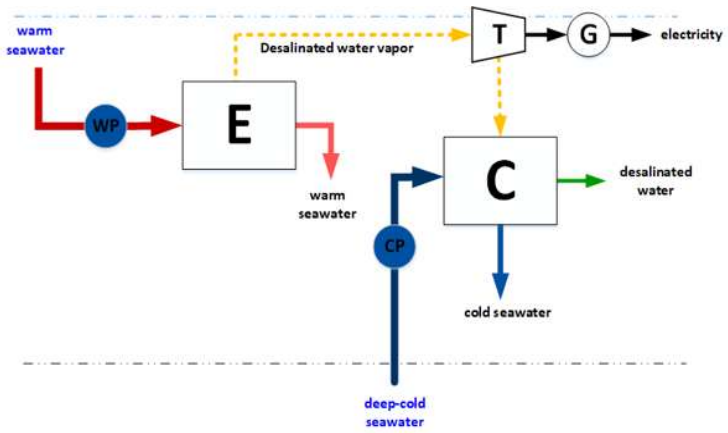

Fig. 1 Offshore open-cycle OTEC plant schematic.

OTEC systems present different advantages that make their analysis attractive and profitable for their development. OTEC system produces renewable energy in a continuous and unlimited way also the operation involves a minimum amount of greenhouse gas emissions. In addition, secondary products obtained from the operation of the OTEC cycles can be achieved, such as air conditioning (Hernández-Romero et al., 2019a), desalinated water (Von Herzen, 2017), and seawater rich in nutrients, which can have another type of potential benefits (Daniel, 1985).

In this sense, different approaches have been developed in order to demonstrate the applications, the electricity generation potential, and the performance of the OTEC system with various working fluids. For example, Nihous (2007) developed a one-dimensional time-domain model for OTECs, where analyzing the great potential for electricity generation, but also the possible damage caused by the large-scale installation of these systems. Hernández-Romero et al. (2019b) analyzed the OTEC cycle as a cooling system considering uncertainty in the energy demand to design and establish the operational policy of the system in a robust way. Another proposal was presented by Gong & Li (2012); evaluated the performance for a closed-OTEC considering different working fluids, of which its performance was evaluated by its capacity of electric generation and its compatibility with the environment. However, the choice of optimum working fluids in the OTEC system will differ depending on the chosen performance indicator.

From the power output viewpoint, R134a high-density organic working fluid is favored according to the study presented by Sauret & Rowlands (2011). Another study that uses the R134a refrigerant as working fluid is presented by Faizal & Ahmed (2013); they performed an experimental study for a closed cycle OTEC system. Since its operation is based on the Rankine thermodynamic cycle, its net power generation and thermal efficiency can be improved by increasing the temperature difference. In this way, Yamada et al. (2009) analyzed the possibility of increasing the efficiency of a solar-boosted OTEC to produce 100kW of power through two proposals, preheating warm seawater to increase its input temperature and superheating the working fluid before it enters a turbine. In addition, as working fluid they used ammonia (NH_3). In addition to this, Aydin et al. (2014) used difluoromethane (R-32) over pure ammonia (NH_3) owing to its non-corrosive, lower toxic

properties and better suitability for superheated cycles. All these studies have in common the conclusion that using both options (Preheating and superheating) improves the gross power thus the efficiency of the system.

From the energetic and exergetic analysis point of view and with optimization focus, different approaches have been developed to improve the analysis and performance of OTEC systems for their implementation. In this context, Sun et al. (2012) propose a theoretical optimization where the net power produced is its objective function as well; they analyzed the performance and exergetic efficiency of the system. Another study was presented by Alamadi et al. (2015) they developed a multi-objective optimization analysis using an evolutionary algorithm to determine the best design parameters for the OTEC system and produce hydrogen. Their analysis consists of minimization of the total cost while the exergetic efficiency is maximized. In the same sense, other studies such as the Jung et al. (2016) have been oriented on the exegetic and thermo-economic analyses of OTEC plants. In this study, they estimate the unit cost of electricity produced by the OTEC system.

However, most of the work considered in the review deals with systems analysis assuming a single energy demand. They do not consider the variation in the energy demands of the end-user along day or year. This factor is key when considering small-scale systems for local production. An inherent advantage of distributed systems is the flexibility of the system to changes in energy demands and habits of the end user (Collins et al., 2017). In addition, OTEC systems are affected by ambient conditions as temperature. It affects exergy efficiency of Rankine cycles as well as the operation of solar collectors. It leads to take into account the variation in solar irradiance for operating solar energy systems (Freeman et al., 2017). A common assumption is to use the highest peak of demand for the design of energy systems. However, it leads to significant gaps between the size of the system and the operational level during low consumption periods or miss-definitions considering interconnected systems (Cardona & Piacentino, 2006).

1.1 OTEC technology: How does it work?

Seawater compared to land, has a higher specific heat, i.e., the amount of heat needed to raise its temperature by one degree is higher. Therefore, it heats up and cools down more slowly than land. However, on land, solar radiation remains almost entirely on the surface, while in seawater, solar radiation penetrates, generally reaching an average depth of one hundred meters, but can spread up to a thousand meters. The penetration of these radiations depends mainly on turbidity, that is, on the amount of solid matter in suspension. All this makes the sea the largest solar collector of solar energy, covering 71% of the earth's surface. In addition, the great thermal inertia of the oceans allows the temperature to be more stable in the oceans and to change less markedly during the course of the day and the four seasons of the year than on the continents. Because of their absorption by the oceans and ocean currents, temperature gradients are produced. The temperature difference between the upper (warm) layer and the lower (cold) layer is in the range of 10°C to 25°C, with higher values found in equatorial waters. When there are large masses at different temperatures, thermodynamic principles predict that an energy-generating cycle can be created that extracts energy from the mass with the higher temperature and transfers an amount to the mass with the lower temperature. Ocean thermal conversion generates electricity on offshore platforms. In tropical seas, temperatures vary from 25°C at the surface to 5°C at 950 m. According to Carnot's principle, if thermal energy is transferred from a hot mass to a cold mass, work is produced and the greater the temperature difference, the greater the amount of energy is produced.

The difference between these energies manifests itself as mechanical energy (to drive a turbine, for example), which can be connected to a generator to produce electricity or used as a cooling medium. In different areas of the world, water has different temperatures depending on its depth (see **Fig. 2**), especially in the tropics, where three thermal layers can be distinguished:

- Surface layer: 100 to 200 meters deep, which acts as a heat collector, with temperatures between 25 and 30 degrees centigrade.

- Intermediate layer: between 200 and 400 meters deep, with a rapid temperature variation and which acts as a thermal barrier between the upper and deep layers.

- Deep layer: where the temperature decreases gently to 4 °C at 1000 meters and 2 °C at 5000 meters.

This huge temperature difference makes the implementation of OTECs possible. The water temperature changes rapidly with depth in the middle region, which is known as the thermocline.

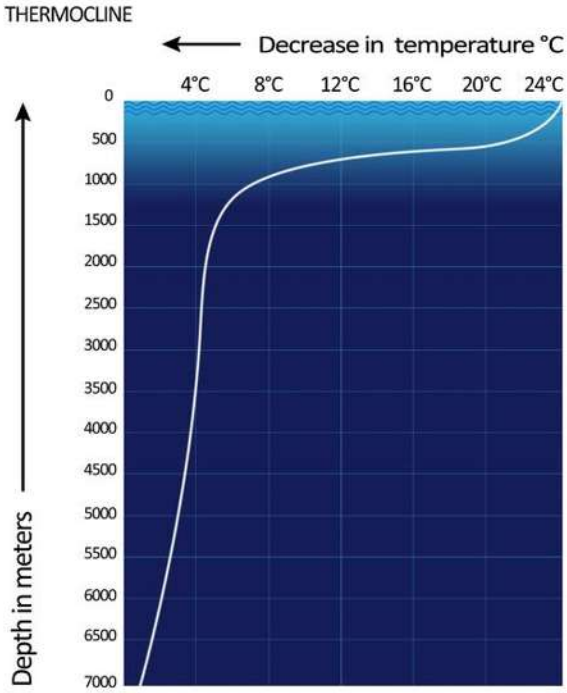

Fig. 2 Thermocline

In addition, solar radiation produces a great heating of the sea surfaces, which reach temperatures of approximately 28ºC. This results in water storing a significant amount of heat energy, since, although this temperature is relatively low, the quantities of water involved are enormous, and the heat absorbed by a body is directly proportional to its mass and the increase in temperature to which it is subjected. In tropical regions, surface seawater can be much warmer than deep seawater. This temperature difference can be used to produce electricity and to desalinate ocean water. Ocean Thermal Energy Conversion (OTEC) systems use a temperature difference to power a turbine to produce electricity. The

temperature difference between the hot seawater flow and the cold-water flow has a strong impact on the efficiency of the system. That is why before implementing a plant, it is necessary for its design to perform meticulous simulations of the operation. It should be noted that in an OTEC plant, the thermal gradient between surface water and deep water must be converted to achieve maximum plant efficiency. The theoretical efficiency of the plant is 8%, when the thermal gradient is of the order of 21°C. In reality, the thermal efficiency obtained is usually between 1 - 3%, and is due to several factors, such as: 1) to obtain a significant amount of energy, large amounts of water flow are needed, and 2). the technology is very sensitive to energy losses.

In this way, the utilization of the thermal gradients of ocean waters is carried out in OTEC plants. In these plants, thermal energy is transformed into electrical energy using a thermodynamic cycle called “Rankine cycle”. Here, the warm surface seawater is pumped through an evaporator containing a working fluid. The vaporized fluid drives a turbine/generator. The vaporized fluid is turned back to a liquid in a condenser cooled with cold ocean water pumped from deeper in the ocean. OTEC systems using seawater as the working fluid can use the condensed water to produce desalinated water.

1.2 By-product from the operation of an OTEC plant

OTEC systems can also supply quantities of cold water as a by-product. This can be used for air conditioning (Seawater air conditioning system “SWAC”) and refrigeration and the nutrient-rich deep ocean water can feed biological technologies. Another by-product is fresh water distilled from the sea (see **Fig. 3**). OTEC has important benefit other than power production, as by product of OTEC, support chilled soil agriculture, aquaculture, fresh water, mariculture and OTEC power plant is not source of environmental pollution.

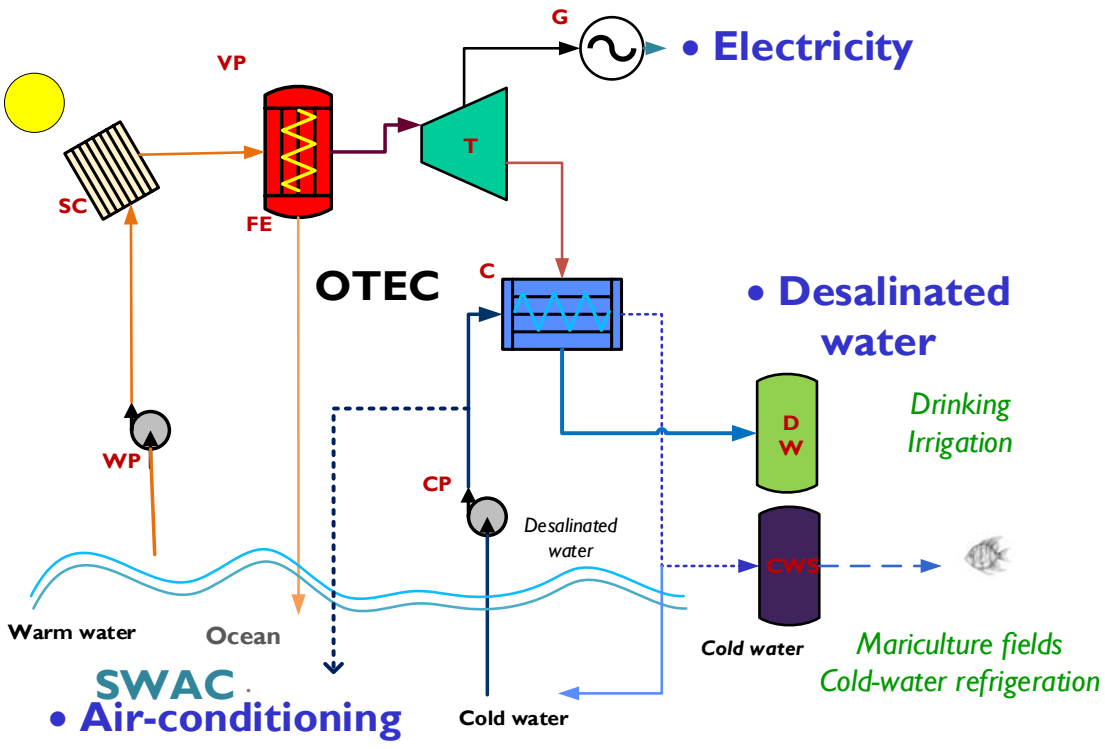

Fig. 3 Open-cycle OTEC plant products

In addition, OTEC plant can generate various benefits:

- **Immense Resource:** OTEC is solar power, using the oceans as a thermal storage system for 24-hour production.
- **Electricity generation:** OTEC produces electricity continuously, 24 hours a day throughout the entire year.
- **Dispatchable Power:** OTEC is dispatchable, meaning that its power can be ramped up and down quickly (in a matter of seconds) to compensate for fluctuating power demand or supply from intermittent renewables.
- **Clean Energy:** OTEC has the potential of being a very clean alternative energy unique for a firm power source capable of providing massive energy needs. The environmental risk with OTEC is very low.
- **Low Risk:** Conventional Closed Cycle OTEC is a low-risk.
- No dependence on fossil fuels or world market fluctuations market fluctuations.

- Generation of nutrient-rich water.
- **Production of fresh water:** Fresh water is the result of the evaporation of sea surface water used as a working fluid (open cycle). Evaporation occurs because the surface seawater is exposed to a partial vacuum process that lowers its boiling point to approximately 23°C, obtaining low-pressure steam.
- **Production of cooling systems** (can save 75% to 85% of air conditioning costs). Cold seawater obtained from the deep sea can provide a large flow rate that allows it to be used to generate conditioned air, even after it has passed through the OTEC plant.

1.3 OTEC potential in Mexico

In Mexico, the main problem to consider is the precise quantification of the availability of marine energy resources and the identification of the sites with the highest thermal potential. Thus, the first technological challenge to be faced is the implementation/improvement of available measurements and data to establish the spatial and temporal variations of ocean energy at a global, national and local scale and to define key sites for the extraction of energy sources. Among the problems, there are also characteristics specific to Mexico that are not necessarily present in other countries. The occurrence of hurricanes, tsunamis, and other extreme events in the sea is of vital importance for technological development. Likewise, the environmental impacts caused by the extraction of energy from the ocean must be evaluated. A major challenge in defining a technology based on clean and renewable energies lies mainly in the use of ocean energy in an environmentally friendly way.

Fig. 4 shows the thermal gradients maps for different zones of the Mexican Pacific, the Caribbean and the Gulf of Mexico taking into account the minimum temperatures and maximum deep-water temperatures. Thermal gradient is equal or greater than 20°C is found from Michoacán to Chiapas. This Pacific zone presents this gradient, since the minimum temperature at a depth of 1000 m is approximately 5°C, while the surface temperature reaches 28°C. In addition, the lowest gradient is found between some area of Michoacán and the Golf of Tehuantepec. There is a small zone within Chiapas that has a greater of up to 21.45°C.

Therefore, using deep cold seawater extraction at 1000 m depth, the states of Michoacán, Guerrero, Oaxaca and Chiapas are the most suitable because they have a thermal gradient equal or greater than 23°C. In this way, Mexico has great potential for developing of this technology.

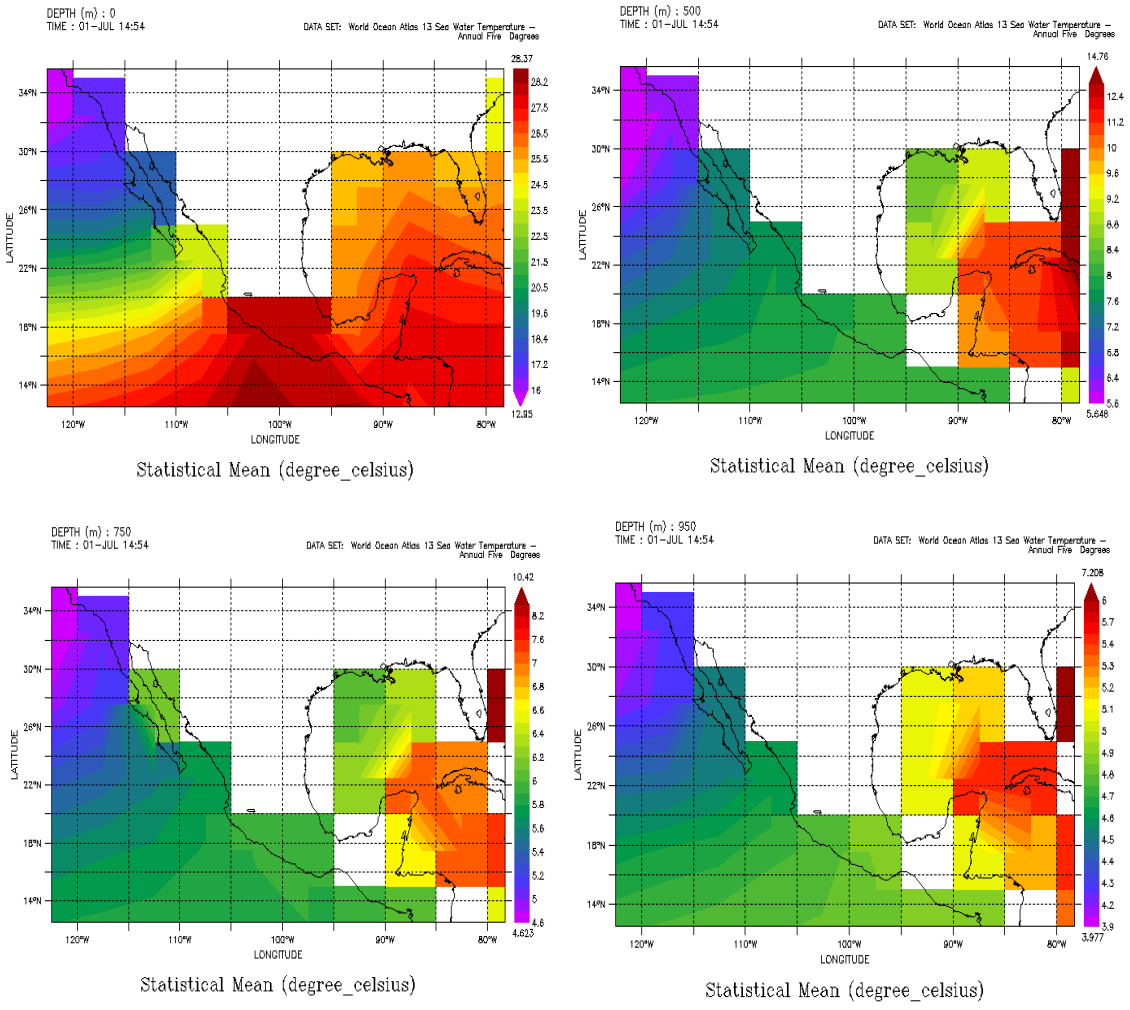

Fig. 4 OTEC potential in Mexico according to the thermal gradient and depth

2. Theoretical Framework

This section is approached in three sections; the first one consists of the general concepts of OTEC plants, their operation and their design. The second section deals with general optimization concepts such as the definition of mathematical model and the development of an optimization problem. The last section deals the different techniques used in this work to address multi-objective problems in the mathematical formulations developed.

2.1 General concepts about OTEC plants

An OTEC (Ocean Thermal Energy Conversion) plant is a power cycle that takes advantage of the ocean's thermal gradient. The ideal geographical area to take advantage of this gradient is between the tropics, where there is a difference of about 20 °C between the surface and 1000 m depth. The cycle operates under a modified Rankine cycle and there can be three different variants of the cycle, which are closed cycle, open cycle and hybrid cycle.

Closed cycle.

The closed-OTEC cycle is a power cycle presented in **Fig. 5**. It consists of a working fluid holding in a closed circuit that alternately evaporates and condenses. In this case, R-134 refrigerant is selected to analyze the cycle. Warm seawater is extracted from the ocean surface at approximately 25°C; this water is directed to a solar collector in order to increase its temperature before entering the evaporator and in this way, taking advantage of the available solar irradiation. Now, in the evaporator, the hot seawater coming from the solar collector will be the fluid with the higher temperature and will transfer heat to the working fluid with a low boiling point(-26.3°C, R134a) (Nithesh & Chatterjee 2016) producing sudden evaporation getting an overheated vapor. Meanwhile, the thermal energy entering the turbine as vapor produces mechanical work and consequently with the help of a generator produces electricity. Pressure and temperature decreases in this process. After that, the low-pressure steam coming out of the turbine must be condensed using deep-cold seawater at approximately 4°C, resulting in a phase change. Subsequently, a pump is responsible for increasing the pressure of the fluid in the liquid phase to reintroduce it back into the evaporator, thus closing the cycle. In this case, the efficiency of the closed cycle is given by

the temperature differential between warm and cold seawater. The bigger temperature difference higher efficiency.

It should be noted that this cycle produces more electricity than the open cycle but does not generate freshwater; the maintenance cost is minimal because the working fluid does not corrode the equipment, with the exception of the evaporator and condenser, and may have a smaller plant size than open cycles (Davis-Morales et al. 2014).

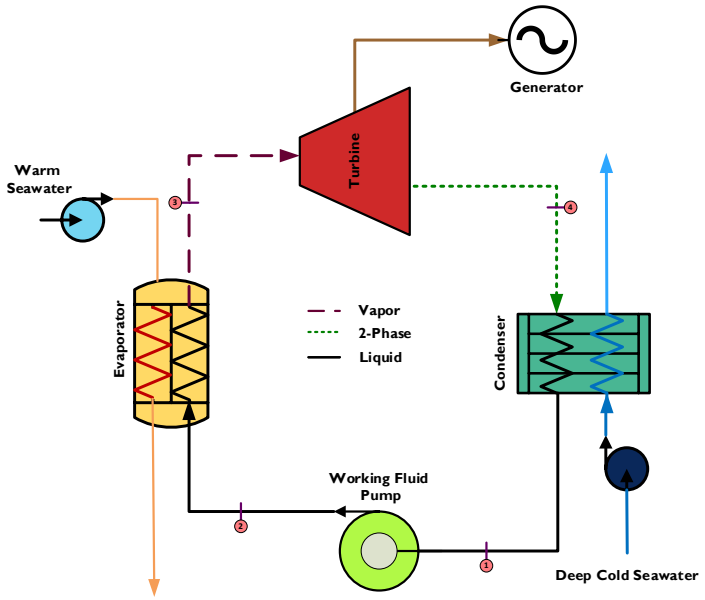

Fig.5. Closed cycle scheme

The operation of closed OTEC cycle follows the thermodynamic cycle shown in **Fig. 6.** According to the T-s diagram, main thermodynamic states are defined by the numbers 1 to 4, 1: saturated liquid, 2: compressed liquid, 3: saturated or overheated vapor and 4: liquid-vapor mixture (wet vapor). In addition, is composed of four main processes.

1-2. Isentropic and adiabatic compression in the working fluid pump. Here, the pressure is increased up to the evaporator pressure value. It implies a power consumption by the pump.

2-3. Heat addition in the evaporator at constant pressure. The saturated vapor enters the evaporator and leaves it as an overheated vapor at state 3.

3-4 An adiabatic expansion of the overheated vapor occurs in the turbine. In this process, the turbine produces work and is connected to a generator to produce electricity.

4-1. High-quality steam is condensed in the condenser using deep cold seawater to a saturated liquid.

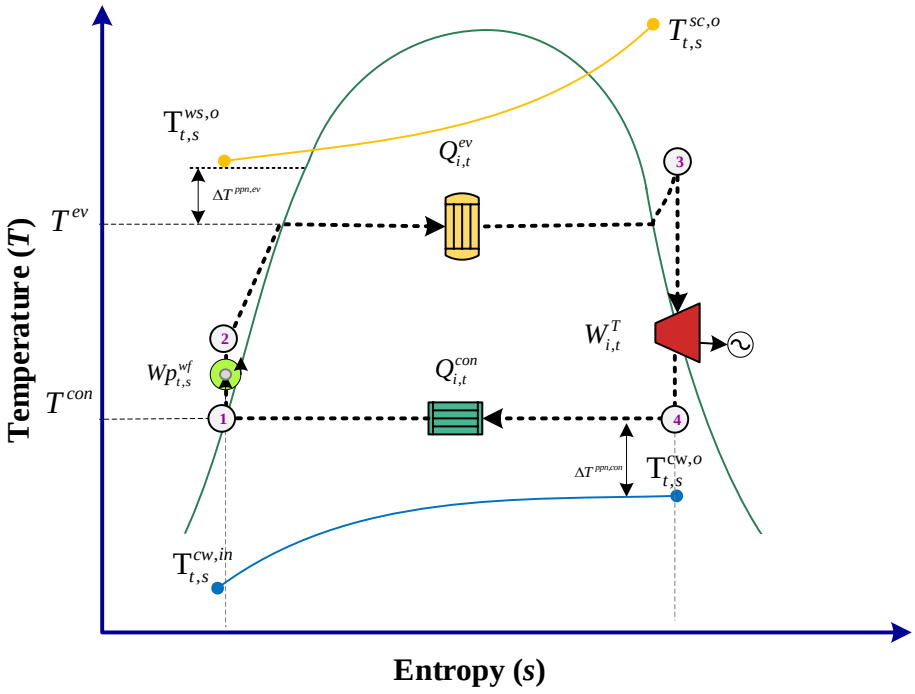

Fig. 6. T-s diagram of closed-cycle OTEC system

Open cycle.

A diagram of the basic open-cycle is presented in **Fig. 7**. Open-cycle OTEC systems utilize surface water warmed by the sun to generate electricity directly. OTEC system has four main components, which are flash evaporator, working fluid, turbine and generator and pumps. In addition, open cycle consists of the following steps:

- Flash evaporation of a fraction of the warm seawater by reduction of pressure below the saturation value corresponding to its temperature
- Expansion of the vapor through turbine to generate power

- Heat transfer to the cold seawater thermal sink resulting in the condensation of the working fluid

Warm seawater at approximately 25°C is extracted from the ocean surface into an evacuated evaporator chamber where the pressure is lower than the saturation condition of the entering seawater. Meanwhile, the thermal energy entering the turbine as steam produces mechanical work and consequently with the help of a generator produces electricity. Pressure and temperature decreases in this process. After that, the low-pressure steam coming out of the turbine must be condensed using deep-cold seawater at approximately 4°C, resulting in a phase change. When exposed to cold deep-ocean water, the steam changes into liquid form, becoming potable. The fresh water can then be used locally for drinking or be processed and shipped elsewhere.

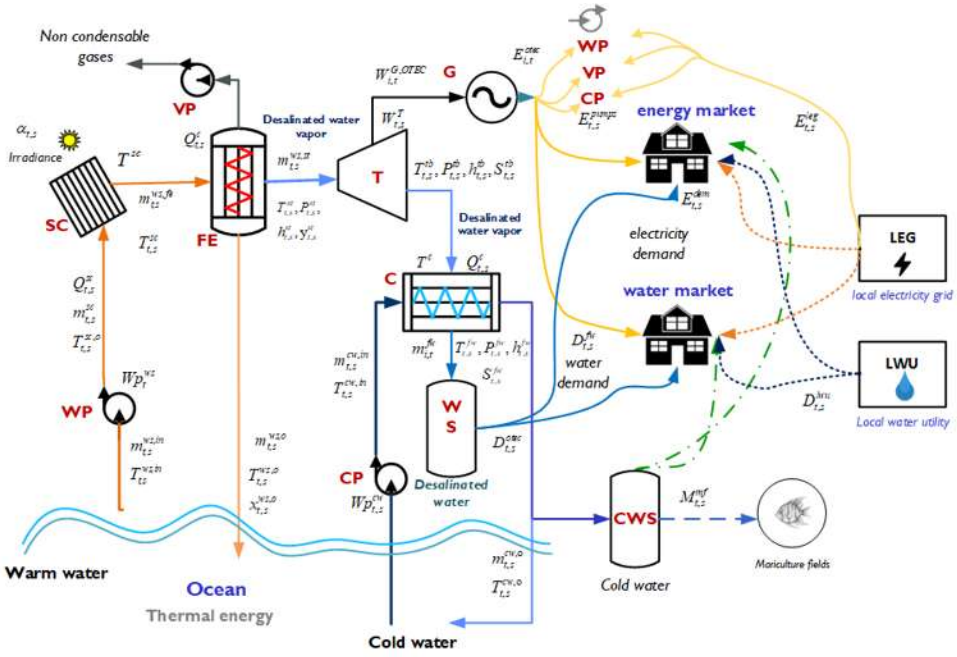

Fig. 7. Open cycle scheme

Fig. 8 shows a Temperature vs. Entropy (T-s) diagram for an open OTEC cycle with the following processes:

1-2. In a vacuum chamber the pressure is reduced in order to reach the boiling point at the inlet temperature of the surface seawater.

2-3. A percentage of salt water is evaporated at constant pressure.

3-4. An adiabatic and reversible expansion of the fluid in the turbine occurs.

4-5. Heat transfer from the working fluid at constant pressure in the condenser.

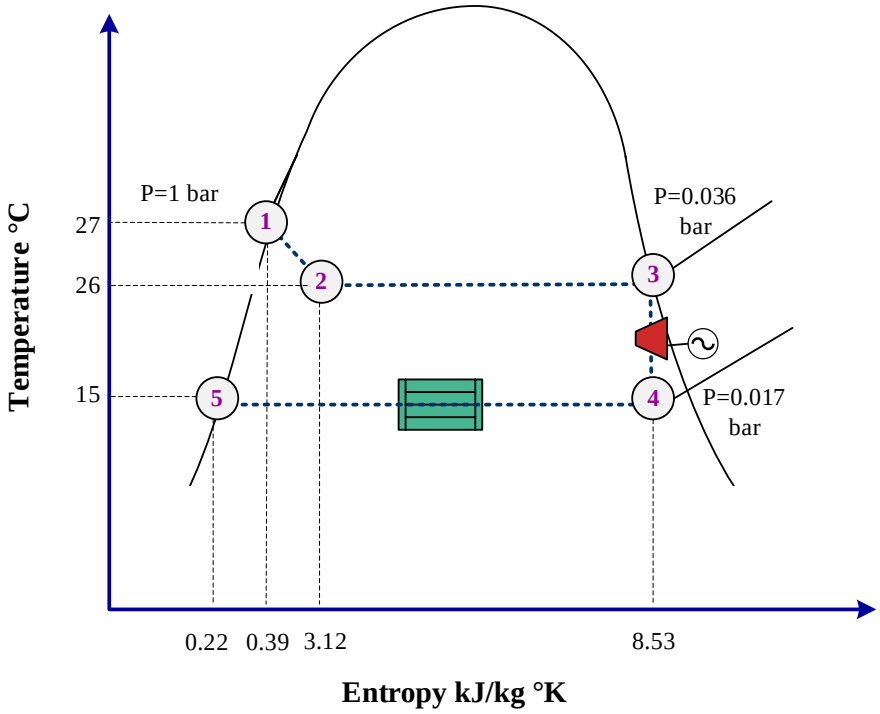

Fig. 8. T-s diagram of open-cycle OTEC system

Hybrid cycle.

The closed-OTEC cycle is a power cycle presented in **Fig. 9**. Hybrid systems combine the characteristics of open and closed cycle systems. A hybrid-cycle ocean thermal energy conversion system contains features from both the above systems using both seawater and a working fluid, usually ammonia. The products obtained from the operation of the hybrid cycle are electricity and desalinated water. In this cycle, the warm seawater enters an evaporator where it is suddenly evaporated (as in the open cycle). The steam obtained from the flash vaporization is used to vaporize the low-boiling working fluid, which operates in the closed cycle. This working fluid steam drives a turbine that produces electricity. In

addition, the steam obtained from the seawater is condensed with the cold deep seawater in a condenser to get desalinated water, which can be used for human consumption, agriculture, etc.

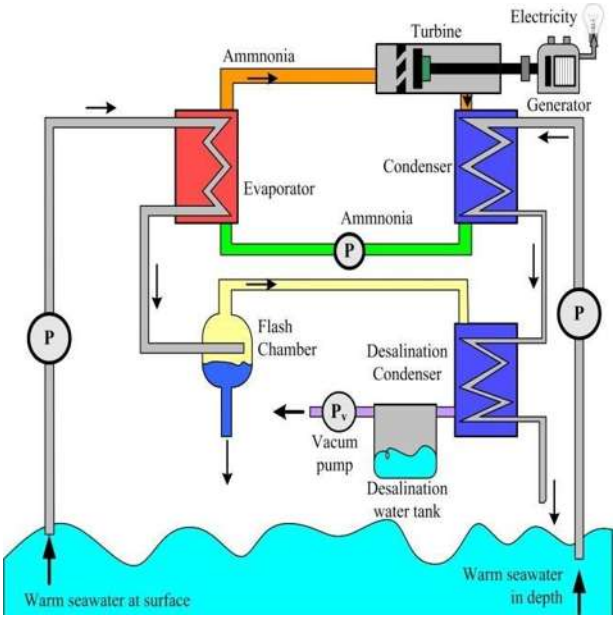

Fig. 9. Hybrid cycle diagram

2.2 Optimization concepts

Modeling

A model is a mathematical representation of the physical chemistry of a determinate process. It is a set of mass and energy balances, thermodynamic relationships, design equations, momentum balances, and particular constraints. Process modeling makes it possible to anticipate and establish benchmarks against which to measure or control the performance of a system.

Mathematical representation of the optimization problem

An optimization problem consists of maximizing or minimizing a real function by systematically choosing input values and computing the function value. An optimization problem consists of defining an objective function, then maximizing or minimizing that

function and thus determining the best values of the design variables. An optimization problem is defined as follows:

$$\begin{aligned} &\text{Min/Max} && f(x) = (x, y) && \text{objective function} \\ &\textit{subject to} && g_j(x) \geq 0, \quad j = 1, 2, \ldots, J && \text{inequality constraints} \\ & && h_k(x) = 0, \quad k = 1, 2, \ldots, K && \text{equality constraints} \\ & && x \in \mathbb{R}^n, y \in \{0,1\} && \text{discrete decisions} \end{aligned}$$

Defining OTEC power cycles as an optimization problem involves different considerations as technical, economic, environmental, security and social considerations. Among the technical considerations is the selection and sizing of equipment for system implementation. The system operation policy, including the operation levels of the generation and energy storage units, are also factors that determine the type and size of technology required. However, the operation policy is determined by aspects beyond the designer's control, such as the level and behavior of energy demand, energy purchase and sale prices in the local energy market, and even environmental conditions. From the economic point of view, the aim is to reduce the cost of the system. Each technology represents different capital costs, efficiencies and operating conditions that affect the economic objective of the system. From an environmental point of view, it seeks to reduce greenhouse gas emissions (GHGE) equivalent to the amount of emissions generated by the use of energy derived from the use of fossil fuels. Socially, the aim is to improve the security of the system, the level of acceptability and the standard of living of the communities, as well as the generation of energy autonomy.

Types of optimization problems

The optimization problem can be mono-objective when there is only one objective function, or multi-objective, when there are several objective functions. In multi-objective problems, one seeks to optimize several objectives at the same time, but in this type of problem, the functions are generally in conflict. In addition, in an optimization problem, the types of mathematical relationships between the objective functions and constraints and the decision variables determine how hard it is to solve, the solution methods or algorithms that

can be used for optimization. According to this, there are different types of optimization problems:

- Linear Programming (LP). The objective function and constraints are linear functions of the independent variables.
- Mixed Integer Linear Programming (MILP). It is a linear programming problem with the existence of integer variables.
- Non-Linear Programming (NLP). At least one objective function or constraint is non-linear.
- Mixed Integer Non-Linear Programming (MINLP). It is a non-linear programming problem with the existence of integer variables.

2.3 Multi-objective optimization strategies

In the development of this work, different solution strategies for multi-objective problems were addressed; in this section, a compilation of these strategies is presented.

Multi-objective optimization (MOO) problems involve two or more optimization goals that are conflicting, meaning that improvement to one objective comes at the expense of another objective. Multi-objective optimization (also known as multi-objective programming, vector optimization, multi-criteria optimization, or Pareto optimization) is an area of multiple-criteria decision-making, concerning mathematical optimization problems involving more than one objective functions to be optimized simultaneously (Chang, 2015). Indeed, in many practical engineering applications, designers are making decisions between conflict objectives, for example, maximizing the efficiency while minimizing total annual cost and emission of a renewable energy system. In these cases, a multi-objective optimization study should be performed, which provides multiple solutions representing the trade-offs among the objective functions. Now, the definition of a multi-objective optimization problem is:

$$\begin{aligned} \underset{x}{\text{Min/Max}} \quad & F_m(x) = \left[F_1(x), F_2(x), ..., F_m(x)\right]^T \quad m = 1, 2, ..., M \\ \textit{subject to} \quad & g_j(x) \geq 0, \qquad j = 1, 2, \ldots, J \\ & h_k(x) = 0, \qquad k = 1, 2, \ldots, K \\ & x_i^{LB} \leq x_i \leq x_i^{UB} \quad i = 1, 2, \ldots, n \end{aligned}$$

Here, m is the number of objective functions; j is the number of inequality constraints and k is the number of equality constraints. $x \in E^n$ is a vector of decision variables; where n is the number of independent variables. $F(x) \in E^k$ represents the objective functions.

Goals in multi-objective optimization

- Find set of solutions as close as possible to Pareto optimal front (see **Fig. 10**)
- Find a set of solutions as diverse as possible.

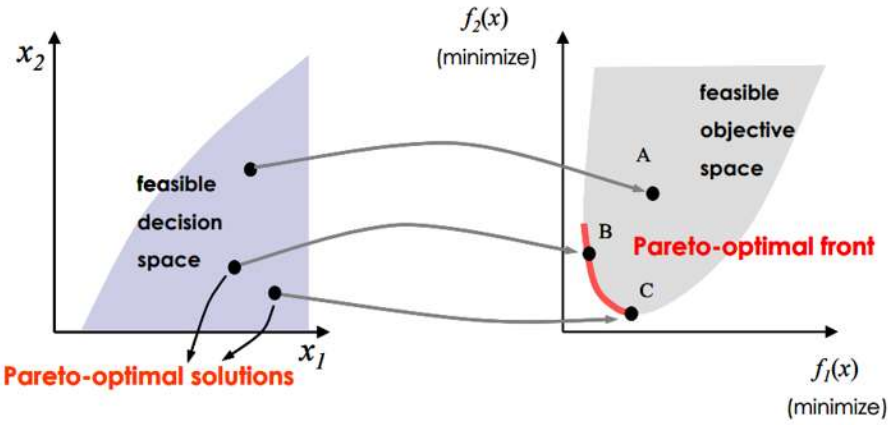

Fig. 10. Graphical description of Pareto Optimal solution

ε-Constrain Method

In the first paper developed in this work, the MOO method selected to solve the problem addressed was ε -Constrain method. This method consist in keep just one of the objective and restricting the rest of the objectives within user-specific values as shown in **Fig. 11**. The mathematical expression to this method is:

$$\text{Minimize} \quad F_{\mu}(x),$$

$$\begin{aligned} \textit{subject to} \quad & F_m(x) \le \varepsilon_m \quad m = 1,2,...,M \quad \textit{and } m \ne \mu \\ & g_j(x) \ge 0, \qquad j = 1,2,\ldots, J \\ & h_k(x) = 0, \qquad k = 1,2,\ldots, K \\ & x_i^{LB} \le x_i \le x_i^{UB} \quad i = 1,2,\ldots, n \end{aligned}$$

In this way, we have two objective functions ($f_1(x), f_2(x)$). The first objective function $f_1(x)$ is considered as a constraint $f_1(x) \le \varepsilon_1$ while keeping $f_2(x)$ as an objective and minimizing it.

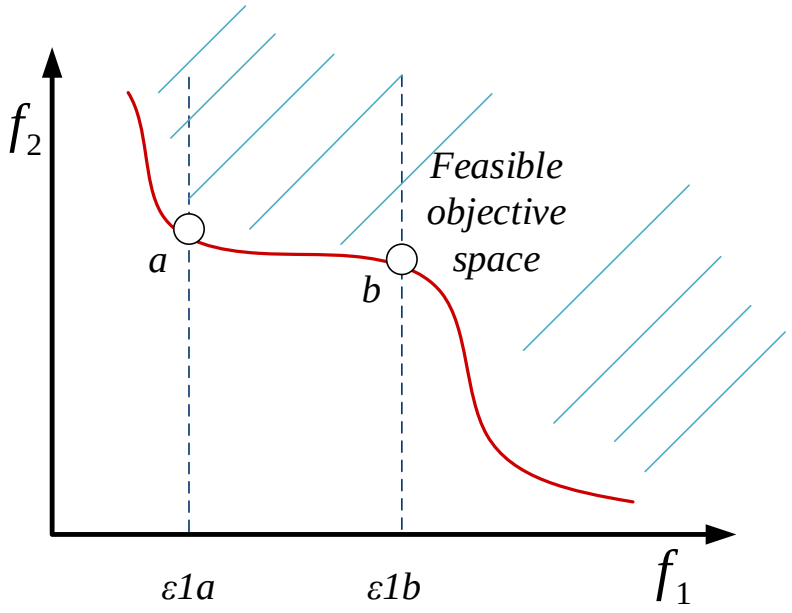

Fig. 11. ε -constraint method diagram

Compromise solution

Compromise solution is based on the point of the utopian solution and it represents a tradeoff between the conflicting objectives. The mathematical formulation of the objective function is performed as follows.

First, objective functions are minimized or maximized according with the interest of the designer. This process allows defining the upper bound (*UB*) and lower bound (*LB*) for the objective functions. These values define the utopia point (*UP*) and the nadir solution (*NS*). The coordinates of the nadir point and the utopian point allow us to scalar the objective

functions and find the solution on the Pareto surface closest to the utopian point; this solution is the compromise solution (see **Fig. 12**).

$$f_i(x) = \left[f_1(x), f_2(x), ..., f_n(x) \right]^T \quad i = 1, 2, ..., n$$

$$\begin{aligned} \textit{subject to} \quad & g_j(x) \geq 0, && j = 1, 2, \ldots, J \\ & h_k(x) = 0, && k = 1, 2, \ldots, K \\ & x_i^{LB} \leq x_i \leq x_i^{UB} && i = 1, 2, \ldots, n \end{aligned}$$

$$\Upsilon_i = \frac{f_i - f_i^{LB}}{f_i^{UB} - f_i^{LB}} \quad i = 1, 2, ..., n$$

$$\textit{Subject to} \ 0 \leq \Upsilon_i \leq 1$$

$$CS = \min \sum_{i=1}^{n} \Upsilon_i$$

Therefore, the compromise solution is defined as the sum of the values of Υ associated to the objective functions.

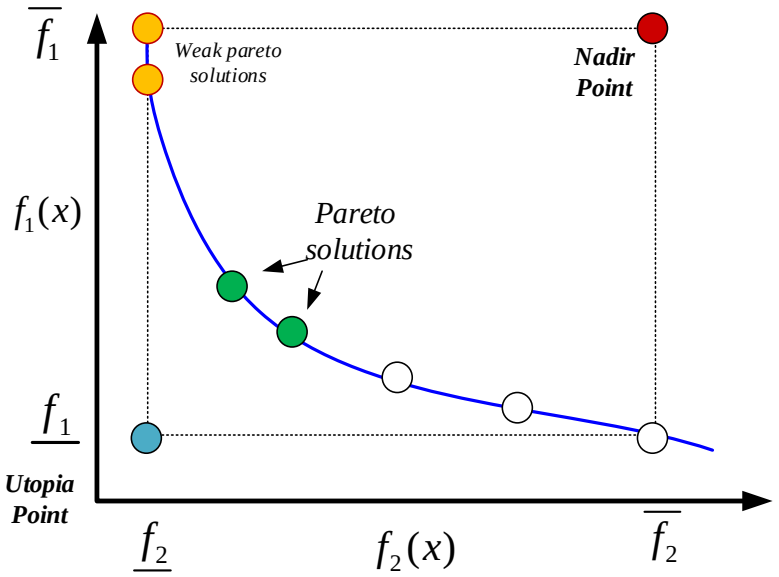

Fig. 12. Compromise solution.

Weighted Sum Method

Fig. 13 shows the weighted sum method. In the weighted sum approach, we scale our set of goals into a single goal by multiplying each of our objectives by a user-supplied weight. The mathematical expression to this method is:

$$\begin{aligned} &\text{Minimize} && F(x) = \sum_{m=1}^{M} w_m f_m(x), \\ &\textit{subject to} && g_j(x) \geq 0, && j = 1, 2, \ldots, J \\ & && h_k(x) = 0, && k = 1, 2, \ldots, K \\ & && x_i^{LB} \leq x_i \leq x_i^{UB} && i = 1, 2, \ldots, n \\ & && \sum_{m=1}^{M} w_m = 1 \end{aligned}$$

In this case, weight of an objective is chosen in proportion to the relative importance of the objective.

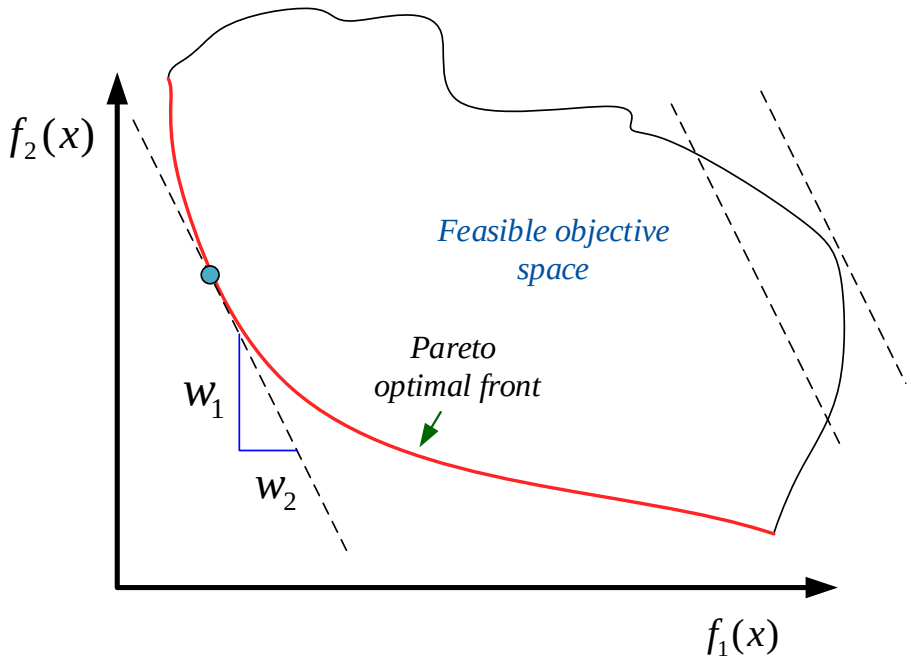

Fig. 13. Weighted sum method.

3. Research Motivation

There are energy and environmental problem of concern due to the increase in the consumption of fossil fuels and the associated greenhouse gas emissions. One of the main contributors to this issue is the generation of energy from hydrocarbons or fossil fuels. However, sustainable alternatives are emerging where it is possible to take advantage of energy from renewable resources such as OTEC systems.

OTEC system is a clean energy source, environmentally sustainable, and capable of providing large amounts of energy. Recently, higher electricity costs increased concerns for global warming and a political commitment to energy security have made the first OTEC commercialization economically attractive in tropical island communities where a high percentage of electricity production is oil-based.

4. Hypothesis

By taking advantage of the temperature gradients between the bottom and the surface of the ocean, it is possible to harness thermal energy with an ocean thermal energy conversion system (OTEC) in its different operating cycles: closed-cycle, open-cycle and hybrid for alternative energy generation. This is intended to reduce the use of hydrocarbons, whose main problem lies in the tons of greenhouse gases they emit into the atmosphere. Therefore, studying and optimizing these systems from a social, economic and environmental point of view can represent alternative solutions to supply the demand for energy and desalinated water to small housing complexes and thus reduce the environmental impact of electricity generation.

5. Objectives

General objective

The general objective of this thesis is to analyze the feasibility of OTEC power cycles in Mexico and developing a mathematical model considering technical, economic, environmental, and social aspects.

Specific objectives

Particularly, the following specific objectives have been considered:

- Propose a formulation to analyze the closed-cycle OTEC system that uses not only ocean thermal energy but also solar-thermal energy.
- The main objective is to determine the size and operational policy of the closed-cycle OTEC system required to supply a given amount of electricity to a housing complex located on the Pacific Ocean coast.
- Determine the optimal technological configuration for the OTEC system implementation.
- Determine the economic, environmental and thermodynamic factors that influence the design of the OTEC systems.
- Determine the system design considering variations in decision variables such as energy demand and surface seawater temperature.

6. Methodology

This section presents the methodology used in development of the research project.

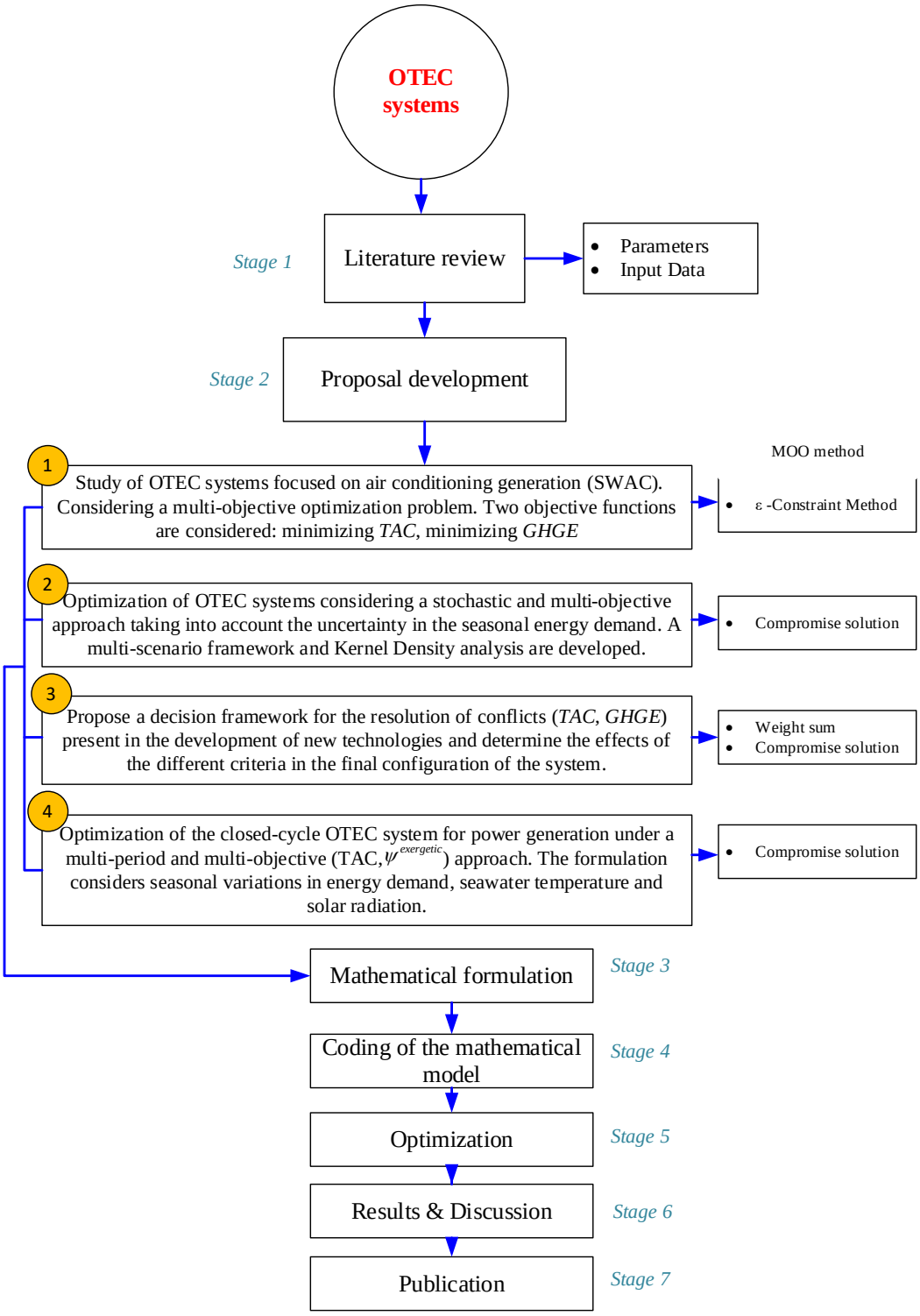

Fig. 14. Sequence diagram.

6.1. Proposal development

Optimal Design of the Ocean Thermal Energy Conversion Systems Involving Weather and Energy Demand Variations.

Ocean thermal energy conversion systems (OTEC) represent an attractive economic alternative in communities allocated in coastal areas for producing electric utilities reducing fossil fuel consumption and emissions. This power generation technology uses the temperature difference between the deep cold water and warm surface water of the ocean to produce electricity using the principles of the Rankine cycle. This chapter presents Non-Linear Programming (NLP) multi-period and multi-objective model for the analysis of OTEC systems. The multi-objective approach consists in to maximize the exergy efficiency of the cycle while the total annual cost of the system is minimized. Variations on solar resources availability, energy demands, and ambient conditions are addressed considering hourly and seasonal profiles from a given housing complex allocated on the Pacific Coast from Mexico.

In this work, the resulting Non-Linear Programming (NLP) model is based on **Fig.15.** The formulation allows analyzing the closed-cycle OTEC system that uses not only ocean thermal energy but also solar-thermal energy. Moreover, R134a is used as working fluid whose choice was based on their thermodynamic and environmental characteristics. A multi-period and multi-objective optimization approach are presented to get the operation policy and sizing of the OTEC plant. For this, the model considers the generation of electricity per hour and per season of the year for a given housing complex as input data. An important consideration that is taken into account is the seasonal variation temperature of surface seawater throughout the year. In addition, the solar radiation is based is taken for the study area and varies based on the time and season. In addition, the model considers the analysis of four important approaches:

- *The thermodynamic analysis*. Here, the status function corresponding to each point of the cycle is adjusted according to the operating temperature and pressure conditions at any given time.

- *Economic assessment*. The economic evaluation is based on the estimation of the costs of the equipment of the system, considering acquisition costs, operating costs and, in certain cases, maintenance costs.
- *Exergetic analysis*. This analysis makes it possible to measure the quality of energy, as well as to evaluate the energy performance of the system.
- *The multi-period and multi-scenario operation of the system*. It results in defining an operational policy according to the changes in ambient conditions and user demand behavior.

Multi-period analysis allows addressing the demand and ambient temperature variations along the day. As presented in the Case Study section, the time resolution considered is hourly. However, it is possible to use different time resolutions according to the criteria of designer and data available. The multi-scenario approach allows considering seasonal variations. Although the approach results in a deterministic model, by considering different scenarios and time variations significant variations can be anticipated. In addition, it is possible to define an operational policy according to the changes in demand and thermal resources, whether solar or oceanic, available.

The multi-objective problem involves two objective functions, where the economic objective must be minimized while the exergy efficiency is maximized. However, it is not possible, since both objectives are conflicting. Therefore, the Epsilon-Constraint Method for solving the multi-objective problem is used to provide a Pareto optimal solution set. In addition, in this work, it is considered that there are no preferences between the conflicting objectives, therefore a compromise solution is proposed for the final solution. It should be noted that such a solution is located somewhere in the middle of the Pareto optimal set.

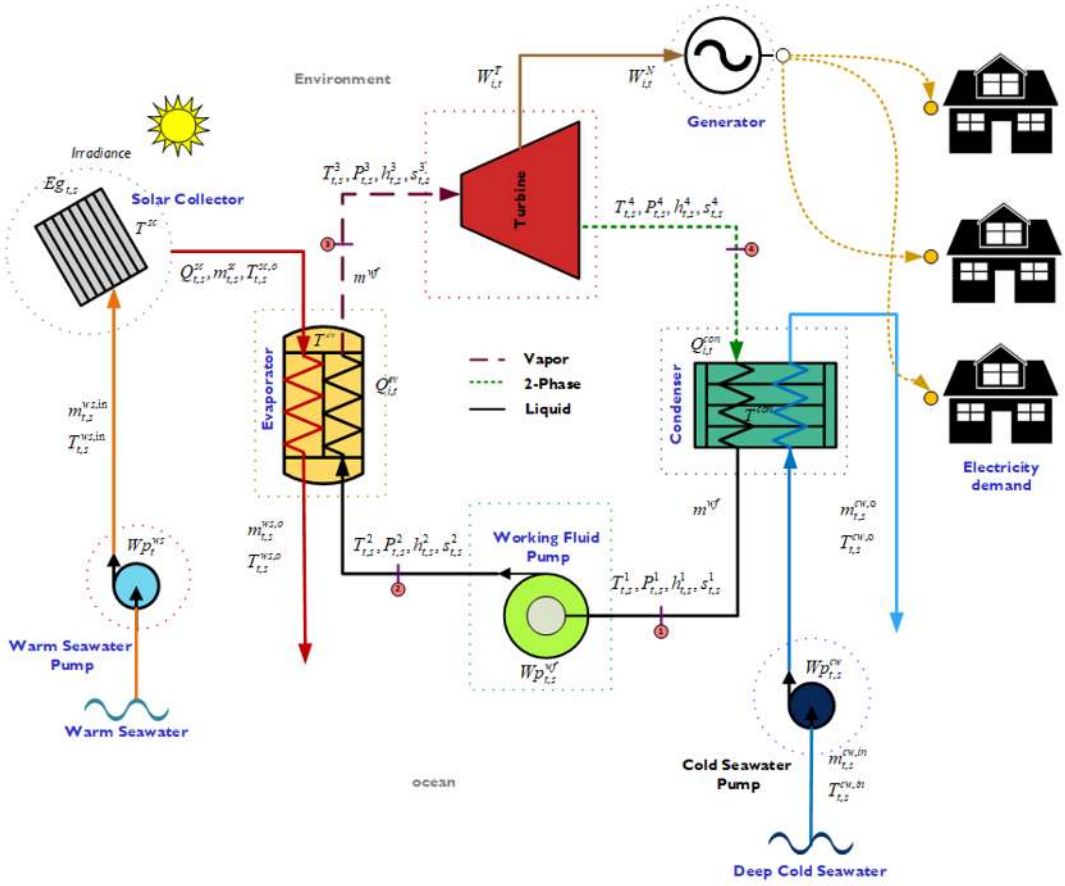

Fig. 15. Proposed diagram for the addressed problem

6.2. Problem statement

The problem addressed in this paper can be stated as follows:

Given are:

- Electricity consumption profile
- Surface-warm seawater temperature seasonal variation profile
- Solar irradiation dataset
- The equipment efficiencies.
- Fixed and variable costs of the equipment.
- Seawater properties
- R134a properties

The problem consists of determining the optimal operating policy and size of the system according to the given electricity requirements that involve thermodynamic, economic and exergetic considerations. In addition, to increase the efficiency of the cycle and to attain low-electricity cost, the average temperature at which heat is transferred to the working fluid in the evaporator must be increased. In this sense, solar energy is considered due to their high performance (Tian & Zhao 2013). Therefore, this work considers the installation of a solar collector to take advantage of solar radiation to increase the temperature of seawater before entering the evaporator. It is worth mentioning that in addition to this, the operational policy considers a multi-period approach and evaluation of the power cycle subject to a set of nonlinear constraints according to time *t* and season *s*. Furthermore, it involves the following:

- The enthalpies, entropies, pressures, and temperatures are calculated according to the thermodynamic state at each point of the cycle.
- Working fluid mass required for the system is obtained.
- Flowrates of warm and cold seawater required by the system.
- Total heat transfer, the total power, and work used by the pumps are estimated.
- Equipment sizing according to the design variables is performed.
- The operational and maintenance required cost to operate the power cycle.
- Calculation of the total exergy flow associated with each input fluid stream.

The problem is addressed as a multi-objective optimization approach that considers minimizing the Total Annual Cost of the system (TAC) while the exergetic efficiency of the system is maximized $\left(\psi^{exergetic}\right)$. The thermodynamic analysis of the process allows establishing the operation policy and sizing of the system based on the electrical requirements by the housing complex. The economic assessment includes the capital costs involving the purchase of all equipment of the system, also the operational costs as well as the maintenance cost of the system. On the other hand, the exergetic objective function involves the thermal performance evaluation of the system.

6.3 Modeling: NLP optimization formulation

This section presents the proposed mathematical model based on the superstructure shown in **Fig.14** to find the optimal operating policy of the closed cycle policy and size of the system. The presented multi-period model consists of the following indexes: *i* represents the time with hour basis (*i=1, 2, 3…24)* and *s* represents the season of the year (*s=spring, summer, fall, winter*). The mathematical formulation is presented in Thermodynamic modeling, Economic Assessment, and Exergy analysis sections and is developed below.

6.3.1. Thermodynamic modelling

6.3.1.1. Solar collector model

Mass balance in the solar collector

A mass balance around the solar collector is carried out; where the extracted warm seawater flowrate from the surface ocean $\left(m_{t,s}^{ws,in}\right)$ will be equal to the mass that enters and exits from the solar collector $\left(m_{t,s}^{sc}\right)$.

$$m_{t,s}^{ws,in} = m_{t,s}^{sc} \qquad \forall t \in T,\ \forall s \in S \tag{1}$$

Energy balance in the solar collector

The energy balance in the solar collector involves the amount of seawater entering and leaving the solar collector $\left(m_{t,s}^{ws,in}, m_{t,s}^{sc}\right)$; the enthalpy of both currents that is a function of the calorific capacity of the seawater $\left(Cp^{sw}\right)$ and as well as its temperatures $\left(T_s^{ws,in}, T_{t,s}^{sc,o}\right)$. In addition, solar energy $\left(Q_{t,s}^{sc}\right)$ is considered:

$$m_{t,s}^{ws,in} Cp^{sw} T_s^{ws,in} + Q_{t,s}^{sc} = m_{t,s}^{sc} Cp^{sw} T_{t,s}^{sc,o} \qquad \forall t \in T,\ \forall s \in S \tag{2}$$

Solar collector design

In this work, a flat plate collector is considered. The Eq. (3) allows estimating the solar thermal energy used by the solar collector that depends directly on the solar collector area $\left(A^{sc}\right)$, solar radiation $\left(Eg_{t,s}\right)$ and efficiency $\left(n_{t,s}^{sc}\right)$ (Trier 2012):

$$Q_{t,s}^{sc} = Eg_{t,s} n_{t,s}^{sc} A^{sc} \qquad \forall t \in T,\ \forall s \in S \tag{3}$$

Where the solar collector yield is given by the following equations:

$$\eta_{t,s}^{sc} = \eta_0 - \frac{\kappa_1 \Delta T}{Eg_{t,s}} - \frac{\kappa_2 \Delta T^2}{Eg_{t,s}} = \eta_0 - \frac{\kappa_1 (\mathrm{T}^m - \mathrm{T}_{t,s}^{am})}{Eg_{t,s}} - \frac{\kappa_2 (\mathrm{T}^m - \mathrm{T}_{t,s}^{am})^2}{Eg_{t,s}} \qquad \forall t \in T,\ \forall s \in S \tag{4}$$

$$T_{t,s}^m = \frac{\left(T_s^{ws,in} + T_{t,s}^{sc,o}\right)}{2} \qquad \forall t \in T,\ \forall s \in S \tag{5}$$

Here, T^m is the mean temperature of solar collector fluid, $T_s^{ws,in}$ is the collector inlet temperature, $T_{t,s}^{sc,o}$ is the collector outlet temperature and $\mathrm{T}_{t,s}^{am}$ is the ambient temperature. In addition, κ_1 and κ_2 are heat loss coefficients while η_0 is the optical efficiency.

It should be noted; that when the differential between the collector and the ambient temperature is zero and the collector loses no energy to the environment the maximum efficiency is achieved.

6.3.1.2. Evaporator model

Mass balance in the evaporator

In the evaporator, the mass that comes from the solar collector $\left(m_{t,s}^{sc}\right)$ is the amount of mass that enters in the evaporator $\left(m_{t,s}^{ev}\right)$ and that will be equal to the mass that comes out $\left(m_{t,s}^{ws,o}\right)$. This is assuming that there are no evaporation losses on contact with the working fluid.

$$m_{t,s}^{sc} = m_{t,s}^{ev} = m_{t,s}^{ws,o} \qquad \forall t \in T,\ \forall s \in S \tag{6}$$

Energy balance in the evaporator

The energy balance corresponds to the heat transfer between hot seawater and the refrigerant working fluid. It can be written as:

$$Q_{t,s}^{ev} = m^{wf} \eta^{ev} (h_{t,s}^3 - h_{t,s}^2) = m_{t,s}^{ev} \mathrm{Cp}^{\mathrm{sw}} (\mathrm{T}_{t,s}^{sc,o} - \mathrm{T}_{t,s}^{ws,o}) \qquad \forall t \in T,\ \forall s \in S \tag{7}$$

In the previous equation, $Q_{t,s}^{ev}$ is the heat transfer rate in the evaporator, m^{wf} is the total mass of the working fluid and η^{ev} is the evaporator efficiency. The enthalpies difference represents the working fluid phase change between states 3 and 1. On the other hand, the temperature difference of the seawater as it passes through the evaporator is taking into account.

Evaporator design

The heat transfer rate is correlated with the overall heat transfer coefficient $\left(U^{ev}\right)$, the mean logarithmic temperature $\left(\Delta Tml_{t,s}^{ev}\right)$ and with the area of the evaporator $\left(A^{ev}\right)$ using Eq. (8):

$$Q_{t,s}^{ev} = U^{ev} A^{ev} \Delta Tml_{t,s}^{ev} \qquad \forall t \in T,\ \forall s \in S \tag{8}$$

Where $\Delta Tml_{t,s}^{ev}$ is given by:

$$\Delta Tml_{t,s}^{ev} = \frac{T_{t,s}^{sc} - T_{t,s}^{ws,o}}{\ln\left[\dfrac{T_{t,s}^{sc} - T_{t,s}^{ev}}{T_{t,s}^{ws,o} - T_{t,s}^{ev}}\right]} \qquad \forall t \in T,\ \forall s \in S \tag{9}$$

Therefore, the heat transfer area of the evaporator is implicitly determined.

6.3.1.3. Turbine model

Turbine power

In the turbine, an isentropic expansion of the working fluid and therefore a pressure drop at the exit of the turbine occurs. The value of power in the turbine $\left(W_{t,s}^{T}\right)$ depends on the working fluid mass m^{wf}, the adiabatic enthalpy difference and as well as the turbine isentropic efficiency $\left(\eta^{T}\right)$ and generator mechanical efficiency $\left(\eta^{G}\right)$.

$$W_{t,s}^{T} = m^{wf} \eta^{T} \eta^{G} (h_{t,s}^{3} - h_{t,s}^{4}) \qquad \forall t \in T,\ \forall s \in S \tag{10}$$

6.3.1.4. Condenser model

Mass balance in the condenser

Assuming there are no seawater losses in contact with the working fluid, the extracted cold seawater $\left(m_{t,s}^{cw,in}\right)$ from the deep ocean required for the condensation is the same is the same amount that comes out of the condenser $\left(m_{t,s}^{\mathrm{cw},o}\right)$.

$$m_{t,s}^{cw,in} = m_{t,s}^{\mathrm{cw},o} \qquad \forall t \in T,\ \forall s \in S \tag{11}$$

Energy balance in the condenser

The energy balance equation at the condenser is the same as the evaporator.

$$Q_{t,s}^{con} = m^{wf}\eta^{con}(h_{t,s}^{4} - h_{t,s}^{1}) = m_{t,s}^{\mathrm{cw},in}\mathrm{Cp}^{\mathrm{sw}}(\mathrm{T}_{t,s}^{\mathrm{cw},o} - \mathrm{T}_{t,s}^{cw,in}) \qquad \forall t \in T,\ \forall s \in S \tag{12}$$

Here, $Q_{t,s}^{con}$ is the heat transfer rate in the condenser, as well as the enthalpies difference represents the working fluid phase change between states 4 and 1. Additionally, the temperature difference of the seawater as it passes through the condenser is required.

Condenser design

The design equations are the same as in the evaporator case. Therefore, the condenser design is given by the following equations:

$$Q_{t,s}^{con} = U^{con}A^{con}\Delta Tml_{t,s}^{con} \qquad \forall t \in T,\ \forall s \in S \tag{13}$$

$$\Delta Tml_{t,s}^{con} = \frac{T_{t,s}^{cw,o} - T_{t,s}^{cw,in}}{ln\left[\dfrac{T_{t,s}^{con} - T_{t,s}^{cw,in}}{T_{t,s}^{con} - T_{t,s}^{cw,o}}\right]} \qquad \forall t \in T,\ \forall s \in S \tag{14}$$

Where, U^{con}, A^{con} and $\Delta Tml_{t,s}^{con}$ are the overall heat transfer coefficient, the mean logarithmic temperature and the area of the condenser respectively.

6.3.1.5. Pumps model

According to the thermodynamic cycle, once the working fluid is condensed $\left(m^{wf}\right)$, the fluid is pressurized and pumped through the evaporator inlet. The energy balance equation for calculating the working fluid power $\left(Wp_{t,s}^{wf}\right)$ can be written as:

$$Wp_{t,s}^{wf} = \frac{m^{wf}(h_{t,s}^{2} - h_{t,s}^{1})}{\eta^{p}\eta^{M}} \qquad \forall t \in T,\ \forall s \in S \tag{15}$$

In addition, the pump η^{p} and the moto η^{M} efficiencies are considered as a parameter.

It is worth mentioning that two more pumps are used and, in the operation, both consume energy, therefore they should be considered. One is for extracting warm seawater $\left(Wp_{t,s}^{ws}\right)$ and the other for extracting deep-cold seawater $\left(Wp_{t,s}^{cw}\right)$. The pumping power is calculated as shown in Eq. (16) and Eq. (17).

$$Wp_{t,s}^{ws} = \frac{m_{t,s}^{ws,in} g \Delta h}{\eta^{ws}} \qquad \forall t \in T,\ \forall s \in S \tag{16}$$

$$Wp_{t,s}^{cw} = \frac{m_{t,s}^{cw,in} g \Delta h}{\eta^{cw}} \qquad \forall t \in T,\ \forall s \in S \tag{17}$$

The power of both pumps depends on the amount of mass seawater being pumped in each case $\left(m_{t,s}^{ws,in} \text{and } m_{t,s}^{cw,in}\right)$. Also, η^{ws} and η^{cw} are the pumps efficiencies and it is supposed to be the same for both. In addition, g is the gravity and finally, Δh is the total pump head difference of each seawater piping.

6.3.1.6. Net work and efficiency of the cycle

The net power output of the system $\left(W_{t,s}^{N}\right)$ is the sum of the work carried out from the starting point to the end of the cycle path. In other words, the net cycle work will be the difference between the generated powers by the turbine minus the sum of the total power used by all the pumps in the cycle:

$$W_{t,s}^{N} = W_{t,s}^{T} - \left(Wp_{t,s}^{wf} + Wp_{t,s}^{ws} + Wp_{t,s}^{cw}\right) \qquad \forall t \in T,\ \forall s \in S \tag{18}$$

The energy efficiency of the system $\left(\eta^{cycle}\right)$ is defined as the net power output of the system divided by input energy at the evaporator, and can be expressed as:

$$\eta^{cycle} = \frac{W_{t,s}^{N}}{Q_{t,s}^{ev}} \qquad \forall t \in T,\ \forall s \in S \tag{19}$$

Efficiency represents the cycle performance, that is to say, the amount of net power generated related to the heat demand supplied.

6.3.2. Process constraints

It should be noticed that these objective functions are subject to different constraints that cannot be omitted during the optimization; these constraints are mass and energy balances, design constraints as well as the technical constraints to determinate the equipment size. Thus, the following constraints must be included in the formulation:

First, a constraint required limiting the amount of warm and cold seawater at the inlet of the pumps; and it has to be lower than the maximum possible flowrate:

$$m_{t,s}^{ws,in} \leq \mathrm{m}^{\mathrm{ws,max}} \qquad \forall t \in T,\ \forall s \in S \tag{20}$$

$$m_{t,s}^{cw,in} \leq \mathrm{m}^{\mathrm{cw,max}} \qquad \forall t \in T,\ \forall s \in S \tag{21}$$

The following restrictions are necessary to determine the size of the evaporator, condenser and solar collector, and with this, it is possible to estimate the cost of each equipment.

$$Q^{sc,max} \geq Q_{t,s}^{sc} \qquad \forall t \in T,\ \forall s \in S \tag{22}$$

$$Q^{ev,max} \geq Q_{t,s}^{ev} \qquad \forall t \in T,\ \forall s \in S \tag{23}$$

$$Q^{con,max} \geq Q_{t,s}^{con} \qquad \forall t \in T,\ \forall s \in S \tag{24}$$

The pinch-point temperature difference in evaporator $\left(\Delta T^{ppn,ev}\right)$ is defined as the minimum temperature difference between the working fluid and warm seawater as well as the pinch-point temperature difference in condenser $\left(\Delta T^{ppn,\mathrm{con}}\right)$ is defined as the minimum temperature difference between the working fluid and cold seawater. Both constraints are needed to allow the exchange between both fluids.

$$T_{t,s}^{ws,o} - T^{ev} \geq \Delta T^{ppn,ev} \tag{25}$$

$$T_{t,s}^{con} - T_{t,s}^{cw,o} \geq \Delta T^{ppn,\text{con}} \tag{26}$$

In addition, a technical constraint must be established to consider an upper bound for the heat transfer in the heat exchangers:

$$\Delta\text{Tml}^{\text{ev,max}} \geq \Delta Tml_{t,s}^{ev} \qquad \forall t \in T,\ \forall s \in S \tag{27}$$

$$\Delta\text{Tml}^{\text{con,max}} \geq \Delta Tml_{t,s}^{con} \qquad \forall t \in T,\ \forall s \in S \tag{28}$$

Turbine and generator sizing is in function of the maximum power generated in all the times.

$$W_{t,s}^{T} \leq \text{W}^{\text{T,max}} \qquad \forall t \in T,\ \forall s \in S \tag{29}$$

$$W_{t,s}^{N} \leq \text{W}^{\text{N,max}} \qquad \forall t \in T,\ \forall s \in S \tag{30}$$

6.3.3. State functions for the R134-a refrigerant

The following correlations are obtained using the Curve Fitting tool in Matlab® software and REFPROP software and as well as the thermodynamic properties of R134a. The change of enthalpy respect to the temperature and pressure for each thermodynamic state and according to **Fig. 3** can be approximated as follow: Z

State 1. Saturated Liquid

Enthalpy (kWh/kg): $h_{t,s}^{1} = 7.143 \cdot 10^{-5} T^{3} - 0.00546 T^{2} + 1.536 T + 199$

Entropy (kJ/kg °K): $S_{t,s}^{1} = 6.06 \cdot 10^{-6} T^{2} + 0.00431 T + 1.006$

Pressure (MPa): $P_{t,s}^{1} = 0.00032 T^{2} - 0.0034 T + 0.3513$

Defining: $dh = Tds + vdP$

State 2. Compressed liquid

Enthalpy (kWh/kg): $h_{t,s}^{2} = h_{t,s}^{1} + v^{1}(P_{t,s}^{2} - P_{t,s}^{1})$

State 3. Overheated vapor (Pressure 1-1.6Mpa)

Enthalpy (kWh/kg): $h_{t,s}^{3} = 400.6 + 0.9337\,\text{T} - 20.99\,\text{P} + 0.00023 T^{2} + 0.0783 TP$

Entropy (kJ/kg °K): $S_{t,s}^{3} = 1.173 + 0.003084T - 0.115P - 2.5 \cdot 10^{-6} T^{2} + 0.00022PT$

State 4. Liquid-vapor mixture

Enthalpy (kWh/kg): $h_{t,s}^{4} = h_{t,s}^{1} + (T + T_{rf}) \cdot (S_{t,s}^{4} - S_{t,s}^{1})$

Where, T_{rf} is the reference temperature.

Here, T is in °C and P is in MPa.

6.3.4. Economic Assessment

The economic evaluation is based on the analysis of capital costs $(CCOST)$, equipment operation $(OCOST)$ and system maintenance $(MCOST)$. Another economic focus consists of the sale of electricity to the residents of the selected housing complex. Capital costs are defined by the fixed costs (FC) represented by the purchase of the equipment and the variable costs (VC) associated with the design variable for sizing the equipment. In addition, it represents the scale parameter, whose function is to adjust the capital cost of the equipment according to the size, (k_F) is the factor used to annualize the capital costs and (H_Y) corresponds to the hours of operation. The costs associated with each equipment are presented below:

6.3.4.1. Solar collector cost

The cost associated with the solar collector considers a flat plate solar collector used to increase the efficiency of the system. In addition, the operational cost of the solar collector is considered:

$$CCOST^{sc} = k_F \left(FC^{sc} + VC^{sc} \left(A^{sc} \right)^{\delta^{sc}} \right) \tag{31}$$

$$OCOST^{sc} = H_Y \left(Cu^{sc} A^{sc} \left(Q^{sc,av} \right)^{\delta^{sc}} \right) \tag{32}$$

Here, $Q^{sc,av}$ is the heat average in the solar collector and Cu^{sc} is the operation unitary cost.

6.3.4.2. Evaporator and condenser cost

The evaporator and condenser costs are associated with the calculated area and are estimated with the following equations:

$$CCOST^{ev} = k_F\left(VC^{ev}\left(A^{ev}\right)^{\delta^{ev}}\right) \tag{33}$$

$$CCOST^{con} = k_F\left(VC^{con}\left(A^{con}\right)^{\delta^{con}}\right) \tag{34}$$

6.3.4.3. Turbine cost

In this sense, the cost associated with the purchase of the turbine depends on the maximum power required by the cycle, and it is estimated as follows:

$$CCOST^{T} = k_F\left(VC^{T}\left(W^{\mathrm{T,max}}\right)^{\delta^{T}}\right) \tag{35}$$

6.3.4.4. Piping and pumps costs

Two main pipe segments are considered. The first segment corresponds to the longest pipe used to extract cold deep-sea water from the ocean $\left(pp^{cw}\right)$, while the second segment of pipe is required to extract hot seawater from the surface $\left(pp^{ws}\right)$.Therefore; the total cost of piping is expressed by the following expression:

$$CCOST^{pp} = k_F\left(pp^{ws} + pp^{cw}\right) = k_F\left(kmL^{ws}\left(D^{ws}\right)^{v} + kmL^{cw}\left(D^{cw}\right)^{v}\right) \tag{36}$$

The piping cost are associated with the length (L) and diameter (D) of the piping, as well as km and v are design parameters that depend on the pipe material.

The total cost associated with the pumps is a function of the maximum amount of seawater pumped in each segment of the pipeline as follows:

$$CCOST^{ws} = k_F\left(FC^{ws} + VC^{ws}\left(\mathrm{m}^{\mathrm{ws,max}}\right)^{\delta^{ws}}\right) \tag{37}$$

$$CCOST^{cw} = k_F\left(FC^{cw} + VC^{cw}\left(\mathrm{m}^{\mathrm{cw,max}}\right)^{\delta^{cw}}\right) \tag{38}$$

In addition, the working fluid pump cost is calculated considering the maximum power in all the times $\left(Wp^{wf,\max}\right)$:

$$CCOST^{wf} = k_F\left(VC^{wf}\left(Wp^{wf,\max}\right)^{\delta^{wf}}\right) \tag{39}$$

6.3.4.5. Generator cost

The cost of the generator is determinate by the maximum net power generated by the cycle $\left(W^{\mathrm{N,max}}\right)$ and is calculated as follows:

$$CCOST^{G} = k_F\left(VC^{G}\left(W^{\mathrm{N,max}}\right)\right) \tag{40}$$

6.3.4.6. Pumping Cost

The pumping cost can be estimated with the following equations:

$$OCOST_{t,s}^{PPC,wf} = \left(PPC_{t,s}^{wf} m^{wf}\right) \quad \forall t \in T,\ \forall s \in S \tag{41}$$

$$OCOST_{t,s}^{PPC,ws} = \left(PPC_{t,s}^{ws} m_{t,s}^{ws,in}\right) \quad \forall t \in T,\ \forall s \in S \tag{42}$$

$$OCOST_{t,s}^{PPC,cw} = \left(PPC_{t,s}^{cw} m_{t,s}^{cw,in}\right) \quad \forall t \in T,\ \forall s \in S \tag{43}$$

Where the parameter (PPC) is the pumping cost parameter and it depends on the amount of seawater or working fluid pumped. Furthermore, this parameter is in a function of the electricity price per kWh (EP), friction factor (f), length and diameter pipeline (L, D) and as well as the pump efficiency $\left(\eta^{ws,cw,\mathrm{wf}}\right)$ of each segment. All of them are related by Eq. (44):

$$PPC = \frac{1}{0.0000576} f \frac{L}{D} \frac{(No.\text{hours})(\mathrm{EP})}{\eta^{ws,cw,\mathrm{wf}}} \tag{44}$$

6.3.4.7. Maintenance of the system cost

The maintenance cost associating with the equipment cleaning to avoid incrustations that could affect the performance of the system. The total maintenance cost is calculated with the

unitary cost per maintenance $\left(U^{ma}\right)$ multiplied by the number of scheduled maintenances per year $\left(\mathrm{NM}^{ma}\right)$.

$$MCOST^{ma} = U^{ma}(\mathrm{NM}^{ma}) \tag{45}$$

6.3.4.8. Refrigerant cost

The refrigerant cost is associated with the amount of working fluid mass $\left(mwf\right)$ required by the plant multiplied by the unitary cost per kg of refrigerant $\left(UC^{wf}\right)$.

$$CCOST^{wf} = UC^{wf} \cdot mwf \tag{46}$$

6.3.5 Exergetic Analysis

The exergy analysis allows achieving efficient and effective use of energy. It can be used for many processes such as power generation. The exergy components are kinetic exergy, potential exergy, chemical exergy and physic exergy (Kotas 1980). However, in this work, the first three are assumed negligible. Equations 47-49 presents the physical exergy

The total flow of physical exergy associated with a current of fluid is:

$$\dot{E}x_{t,s}^{ws,in} = m_{t,s}^{ws,in}\left[\left(h_{t,s}^{ws,in} - ho\right) - To\left(S_{t,s}^{ws,in} - So\right)\right] \qquad \forall t \in T,\ \forall s \in S \tag{47}$$

$$\dot{E}x_{t,s}^{cw,in} = m_{t,s}^{cw,in}\left[\left(h_{t,s}^{cw,in} - ho\right) - To\left(S_{t,s}^{cw,in} - So\right)\right] \qquad \forall t \in T,\ \forall s \in S \tag{48}$$

$$\dot{E}x_{t,s}^{sc} = m_{t,s}^{sc}\left[\left(h_{t,s}^{sc} - ho\right) - To\left(S_{t,s}^{sc} - So\right)\right] \qquad \forall t \in T,\ \forall s \in S \tag{49}$$

Where ho and So are the specific enthalpy and specific entropy respectively at dead state. Here, the reference dead state is assumed as same as ambient conditions $To = 298.15°K$ and $Po = 101.3\,kPa$ (Rosen & Dincer 2004).

Therefore, the total exergy of the system in time *t* and season *s* is:

$$\dot{E}x_{t,s} = \dot{E}x_{t,s}^{ws,in} + \dot{E}x_{t,s}^{cw,in} + \dot{E}x_{t,s}^{sc} \qquad \forall t \in T,\ \forall s \in S \tag{50}$$

6.4. Multi-objective Approach

6.4.1. ε -Constraint Method.

The multi-objective formulation seeks to maximize the total exergy efficiency $\left(\psi^{exergetic}\right)$ considering the Total Annual Cost of the system $\left(TAC\right)$ that will be minimized simultaneously. The ε-Constrain Method is applied to addressed thus problem, where the solution of a set of several single optimization problems for minimizing the *TAC* under upper constraint for the $\psi^{exergetic}$ yields a set of Pareto optimal solutions that compensate the considered objectives.

$$F = MinTAC + Max\psi^{exergetic} \tag{51}$$

s.t $\psi^{exergetic} \leq \varepsilon$

The objective functions considered in this problem are presented as following:

6.4.2. Economic function

The economic objective function consists in the minimization of the Total Annual Cost $\left(TAC\right)$ of the process considering the capital costs $\left(CCOST\right)$, operational costs $\left(OCOST\right)$, and maintenance cost of the system $\left(MCOST\right)$ through the economic evaluation of all components of the cycle $\left(n\right)$: turbine, generator, evaporator, condenser, pumps, piping, solar collector. Thus, the TAC is calculated as follows:

$$TAC = \sum_{n=1}^{N}\left(CCOST + OCOST + MCOST\right) \tag{52}$$

6.4.3. Exergetic function

The second law efficiency or also called exergetic efficiency $\left(\psi^{exergetic}\right)$ can be expressed as the relationship between the outputs of useful exergy produced $\left(W^{N}\right)$ and consumed $\left(\dot{E}x\right)$ (Lozano &Valero 1993). Therefore, the second objective function is the exergetic efficiency and is written as follows:

$$\psi^{exergetic} = \frac{W^N}{\dot{E}x} \tag{53}$$

6.4.4 Compromise solution

A compromise solution is a solution that is located somewhere in the middle of the Pareto optimal set. When there are no preferences between conflicting objectives, a compromise solution can represent the final solution. Therefore, the compromise solution is defined as one that achieves a suitable trade-off between the both objectives. The compromise solution will be the one closest to the utopian point (Marler & Arora 2004). In order to be able to compare both objectives, the objective functions must be scaled using variable Υ :

$$\Upsilon_1 = \frac{TAC - TAC^{LB}}{TAC^{UB} - TAC^{LB}} \tag{54}$$

$$\Upsilon_2 = \frac{\psi^{exergetic} - \psi^{exergeticLB}}{\psi^{exergeticUB} - \psi^{exergeticLB}} \tag{55}$$

St. $0 \leq \Upsilon_1, \Upsilon_2 \leq 1$

Where, the utopia point ($TAC^{LB}, \psi^{exergeticUB}$) are obtained from solved independently each objective function. However, it corresponds to an infeasible solution, because the two objectives are in conflict. In addition, the solution of the objectives also defines the coordinates of the nadir point ($TAC^{UB}, \psi^{exergeticLB}$), which define the coordinates of the nadir point. The coordinates of the nadir point and the utopia point allow us to scale the objective functions and find the solution on the Pareto front that is closest to the utopia point. This solution is the compromise solution (CS).

Therefore, the compromise solution (CS) results from minimizing the difference between the set of normalized objective functions, as one objective function is minimized while the other is maximized.

$$minCS = \left|\Upsilon_1 - \Upsilon_2\right| \tag{56}$$

7. Case study

A case study for a certain housing complex located in Lazaro Cardenas, Michoacán is presented to apply the proposed model. Different input information is required to feed the model. In this case, a seasonal electricity consumption profile per hour for the selected housing complex is given and is shown in **Fig. 16**. As observed, peak consumption, periods occur along the day, but they are remarkable at early morning (6 hrs.) and late night (20 – 22 hrs.)

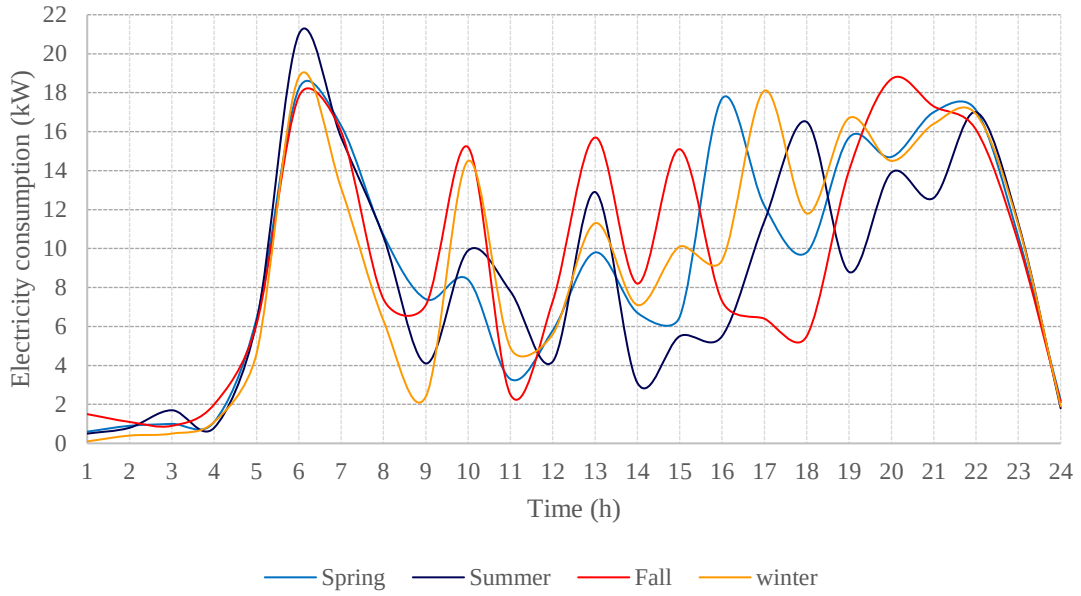

Fig. 16. Electricity consumption profile of a housing complex located in Lazaro Cardenas

On the other hand, in order to increase the cycle efficiency, the use of solar energy is considered in the modeling. **Table 1** shows technical information and efficiencies about the cycle components, ambient conditions as well as parameters used in the modeling.

Table 1. Parameters required for the optimization

Concept	Symbol	Value
Turbine efficiency	η^{Tr}	0.9
Generator efficiency	η^{G}	0.87
Motor efficiency	η^{M}	0.8
Warm and cold seawater pumps efficiencies	η^{ws} , η^{cw}	0.8
Working fluid pump efficiency	η^{wf}	0.75
Evaporator overall heat transfer coefficient	U^{ev}	4 kW/m^2°C
Condenser overall heat transfer coefficient	U^{con}	3.5 kW/m^2°C
Cold Seawater inlet temperature	$T^{cw,in}$	4.5°C
Cold Seawater outlet temperature	$T^{cw,o}$	8°C
Seawater specific heat capacity	Cp^{sw}	0.001109 kWh/Kg°C
Seawater density	ρ^{sw}	1026.56 kg/m^3
Optical efficiency	ηo	0.8
Factor used to annualize the capital costs	k_F	0.463
Warm and cold seawater pipelines diameter	D^{ws}, D^{cw}	0.5 m
Warm seawater pipeline length	L^{ws}	50 m
Cold seawater pipeline length	L^{cw}	950 m
Pinch point in evaporator (Yamada et al. 2016)	$\Delta T^{ppn,ev}$	2°C
Pinch point in condenser (Yamada et al. 2016)	$\Delta T^{ppn,\mathrm{con}}$	1.8°C

Moreover, the seawater-temperature variation respect to the depth for the Lazaro Cardenas coastal is considered (**Fig. 17**). It is important to note that the annual average surface temperature is approximately 28°C and reaching a maximum of up to 30°(see **Fig. 17a)**; while the temperature distribution at a depth of 1000 m ranges is from 4 to 5°C in the area around the selected zone as seen in **Fig. 17b**. It should be noted that the cold seawater that enters the condenser with a value of 4.5°C is fixed. Besides, the seawater temperature of ocean surface varies according to the amount of radiation absorbed by direct exposure in a

given season of the year. In this work, the seawater temperature seasonal variation is considered (**Fig. 18**); also, the figure shows the profile shows the maximum, minimum and average surface temperature for the selected location. In this way, **Fig. 19** shows the corresponding solar irradiation data required for the study area.

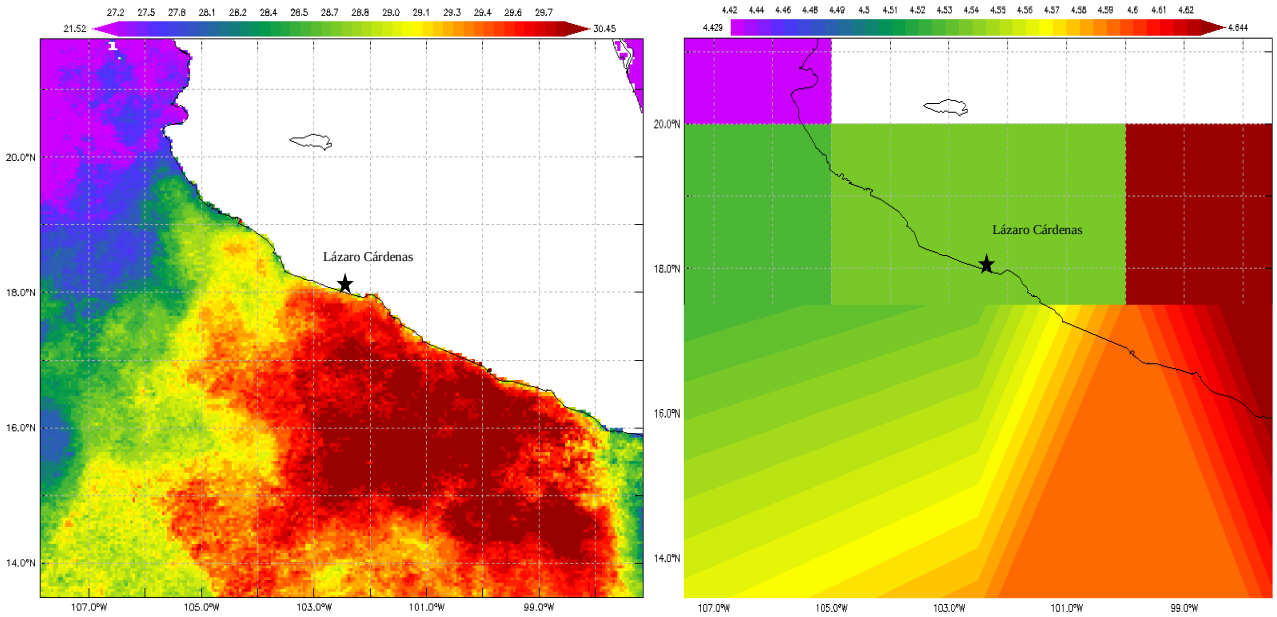

a) Surface seawater temperature b) Deep seawater temperature at 1000m

Fig 17. Seawater-temperature average distribution for Lazaro Cardenas coast (NCEI 2013)

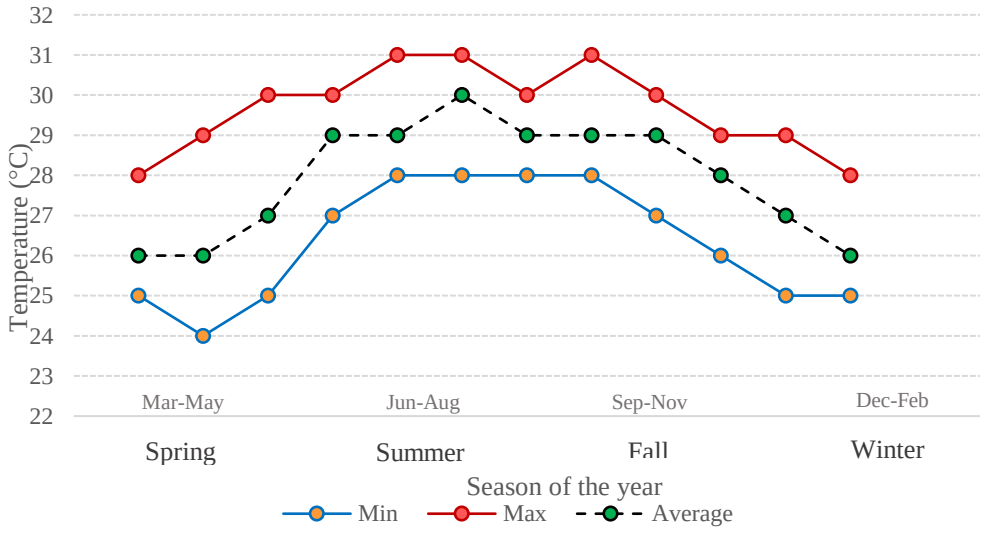

Figure 18. Seawater temperature variation through of the season of the year

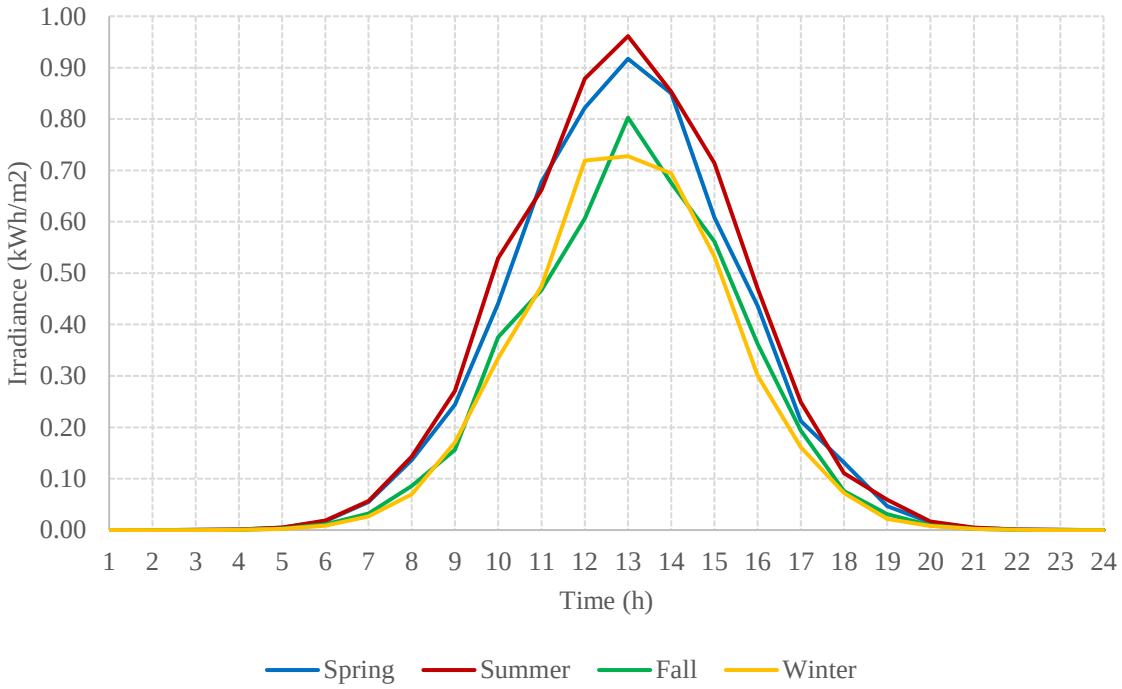

Figure 19. Seasonal solar radiation for Lazaro Cardenas (kWh/m^2)

8. Results

The model was developed under a multi-objective, multi-period optimization formulation. On the other hand, being a non-linear formulation, an initialization strategy was needed. The mathematical model was coded in the GAMS software (Brooke. 2014). It consists of *5019 continuous variables, 5871 constraints and, 4420 nonlinear terms*. The NLP model was solved using BARON solver. The model was solved using the Epsilon-constraint method to obtain the Pareto front (see **Fig. 20**), where each point represents a different solution. The results are presented for three different cases according to the preference of each objective. The first case shows the results when the Total Annual Cost is minimized, the second case corresponds to exergetic efficiency maximization. Finally, a compromise solution to reach a trade-off between both objectives is presented in the third case. The sizing of the equipment and the mass working fluid required for each solution are presented in **Table 2**. **Fig. 20** shows the Pareto sets of optimal solutions for total annual cost versus the maximum exergetic

efficiency of the system. These results clearly indicate that both objectives are in conflict: improving the exergetic objective increases the total annual cost of the system and vice versa.

Point A in **Fig. 20** is the solution from the minimization of the total annual cost (*TAC*). In this case, $98,087/year is obtained while the exergetic efficiency presents a value of 3.5%. Since the objective consists of the minimization of the TAC, the solar collector is not required, as implementation would significantly increase the TAC. Therefore, the configuration of the system and the operational policy, as well as the net cycle efficiency, will depend on the hot source (warm seawater). The area of the evaporator and the condenser is $2m^2$ each. While the working fluid mass required in the system has a value of 420 kg. It is worth mentioning that the mass of refrigerant is in a closed cycle. Moreover, the amount of refrigerant mass required to satisfy the electricity demands is very high since the system sacrifices the amount of refrigerant since it is cheaper instead of the increase of the equipment sizing. Points B, C, D, and E show the trade-offs between the considered objectives. The possible configurations represented by each of the points of the Pareto front represent solutions that can be taken into account in a decision-making framework according to the priorities considered. However, in this work, an equality assumption between both objectives is considered; therefore, a compromise solution is presented in Point C. In Point B, the TAC is $107,896/year with 4.1% exergetic efficiency, this solution increases the TAC by 10% and the $\psi^{exergetic}$ by 0.54% compared with the best economic solution (Point A). In this case, the system requires an evaporator and a condenser of $5m^2$ and $10m^2$ respectively as well as a solar collector of $17m^2$. In addition, this solution involves the use of 435 kg of the working fluid. On the other hand, the Point C solution has a total annual cost of $130,554/year, and the system has an exergetic efficiency of 5.2%. In this case, the system requires an evaporator of 10m2, a condenser of 37 m^2, as well as a solar collector of 92 m^2 and 480 kg of working fluid mass. Here, the solar collector size increase more than five times compared with the Point B solution.

Point E with a TAC of $157,971/year is the worst economic solution whereas the exergetic efficiency is the best with a value of 7.4%. This solution requires evaporator and condenser areas of 13 m^2 and 46 m^2 respectively. While 500 kg of working fluid mass is necessary. In addition to this, the solar collector for maximum energy efficiency is installed prior to the

evaporator, in order to increase the temperature of hot seawater. With an area of 129 m^2 is possible. However, it should be noted that the installation of a solar collector increases the TAC with respect to the required area.

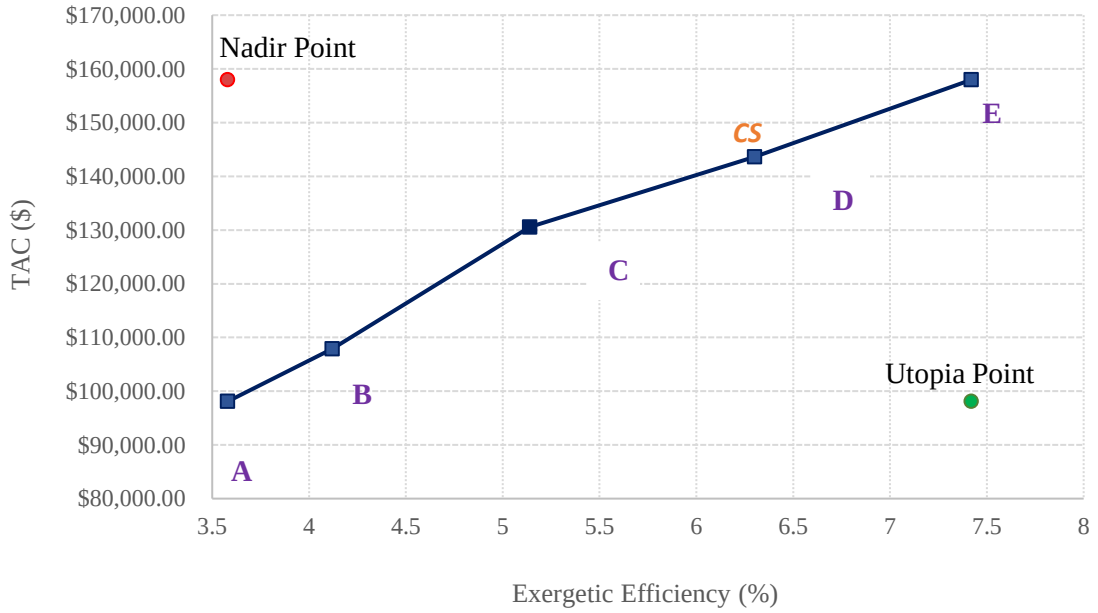

Figure 20. Pareto front

In this way, Point D is the compromise solution, and it was obtained from Eq. (56). The analysis of this solution presents a trade-off between the economic and exergetic efficiency objective. With a TAC of $143,610/year and $\psi^{exergetic}$ with a value of 6.3%. This proposal represents an increase of 46.41% in the TAC compared with the Point A solution and 9.10% less than Point E solution. Respect to the exergetic objective, the $\psi^{exergetic}$ obtained in this solution corresponds 2.8% more with respect Point A and 1.1% less than the best solution. Moreover, the evaporator and condenser areas required by the closed cycle are 13 m^2 and 46 m^2 respectively. To achieve the exergetic efficiency a solar collector with 107m^2 is necessary. The total cost of the system is mainly affected by the size of the solar collector, that is to say, the larger the size the higher the efficiency of the system. On the other hand, the mass of the system is not altered in each of the solutions, since the results show a variation in a range of 80 kg. In addition, the sizes of the condenser evaporator are altered insignificantly compared to the solar collector.

Table 2. Optimization results

Optimization Variable	Point A Min (TAC)	Point B	Point C	Point E Max($\psi^{exergetic}$)	Compromise solution
Solar collector area, m^2	-	17	92	129	107
Evaporator area, m^2	2	5	10	13	13
Condenser area, m^2	2	10	37	46	46
Working fluid mass, kg	420	435	480	500	500
TAC, $	98,087	$107,896	130,554	157,971	$143,610
$\psi^{exergetic}$,%	3.5	4.1	5.2	7.4	6.3

For this solution, **Figs.21-25** shows the operational policy of the system for each time *t* and each season *s*. It worth to mentioning, operational policy satisfies the electricity demand given for a housing complex hour basis. **Fig.21** shows the amount of warm and cold seawater required by the system. Also shows the demand for hot seawater required at each time and by season. In spring and fall, the warm seawater flow is practically constant at all times. While in winter a greater portion of seawater is necessary given that the temperature of seawater is lower, however, in summer the amount of water decreases because the temperature is higher and when entering the collector increases its temperature before entering the evaporator, therefore higher thermal energy is enough to satisfy the electricity demand. In addition, **Fig.21** shows the cold seawater distribution required by the system in the condensation process.

Fig. 16 shows the profile of energy demand for a housing complex by the hour and season of the year. The highest peaks occur at 6 hrs. in spring, summer, and winter while in fall the peak occurs at 20 hrs. In this way and according to **Fig. 21**, the system remains in constant

operation, managing to supply the energy requirements at a given time. In this case, the peaks of energy demand in each of the seasons of the year would imply a change in the operation of the system, hoping that the system has greater seawater requirements to supply them; however, the system is able to keep up a constant operation in the face of high and low energy consumption demands. In summer, as has already been said, the highest peak is 6 hours. However, there is a decrease in hot seawater requirements, this is because the seawater surface reaches high temperatures during the summer, therefore, the temperature at which seawater enters the evaporator is sufficient to generate the amount of steam required to supply the energy demand.

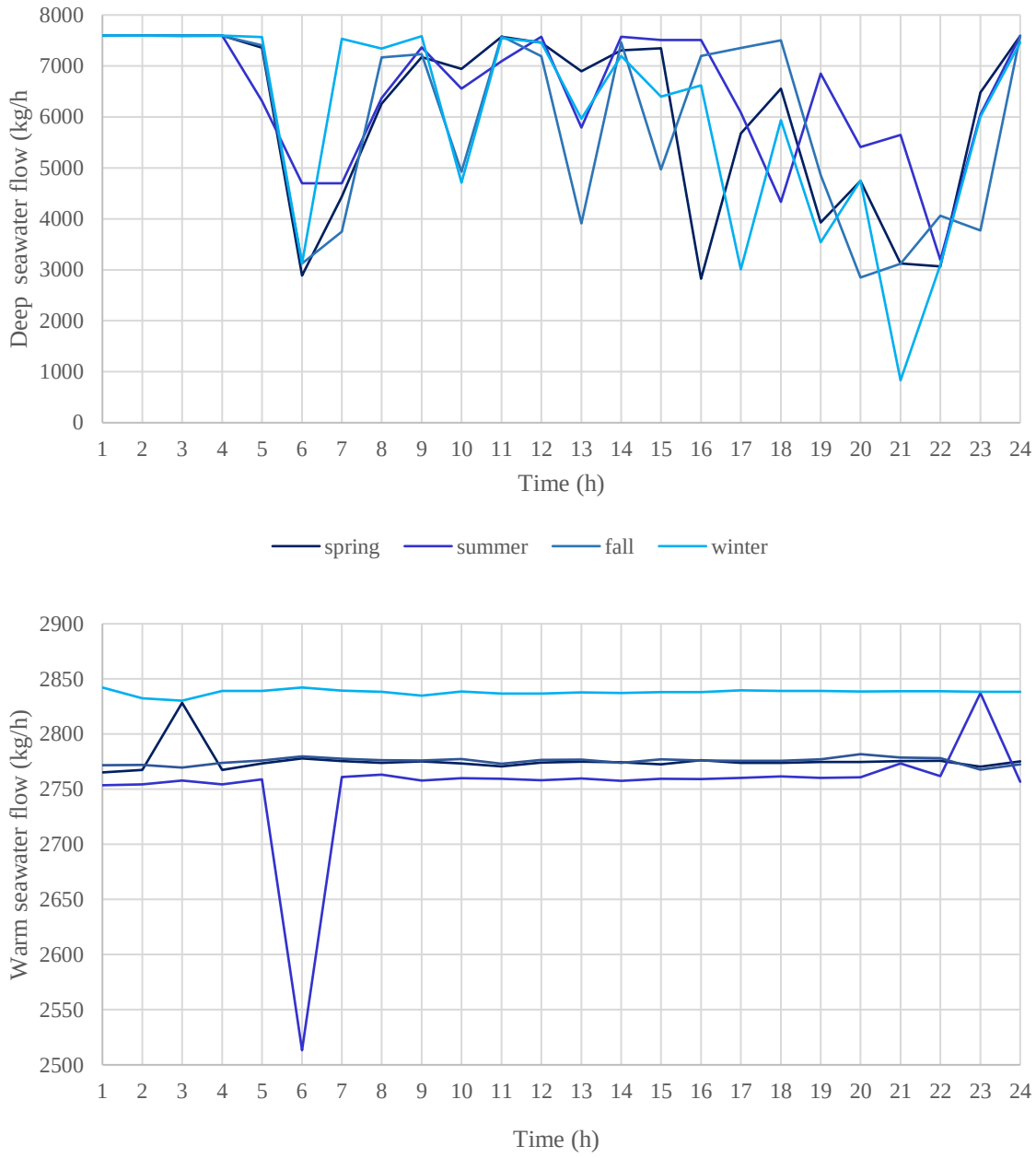

Figure 21. Warm and cold seawater flows per hour per season

Fig. 22 shows the temperature in the solar collector, this temperature is increased by the incident solar radiation, so that seawater at this temperature will be the one entering the evaporator. According to **Fig 19.** Presented above, at certain times (1-5hrs and 21-24 hrs.) there is no solar radiation, therefore, the seawater inlet temperature to the evaporator is the ocean surface temperature. **Fig. 22** shows the temperature profile of the solar collector, where

the temperature reaches values of up to 50°C in summer between 12 and 3 hrs. It also shows the temperature profile of the evaporator and the outlet temperature of the evaporator respectively. In the same sense, the profiles for condenser temperature, condenser inlet, and outlet temperature are presented in **Fig. 22**.

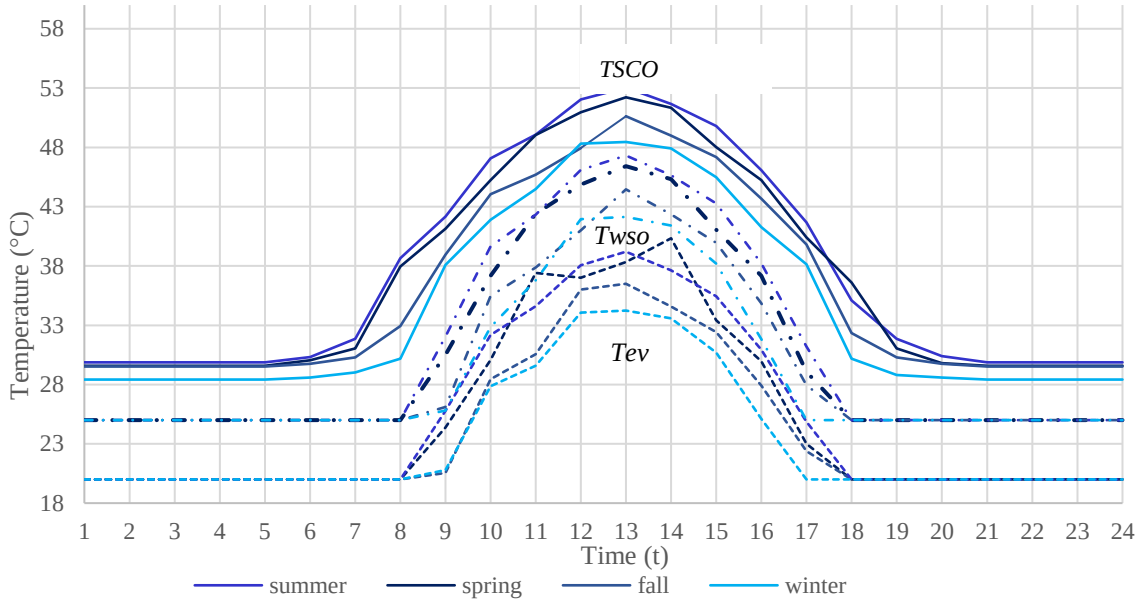

Figure 22. Warm seawater inlet and outlet temperature and evaporator temperature.

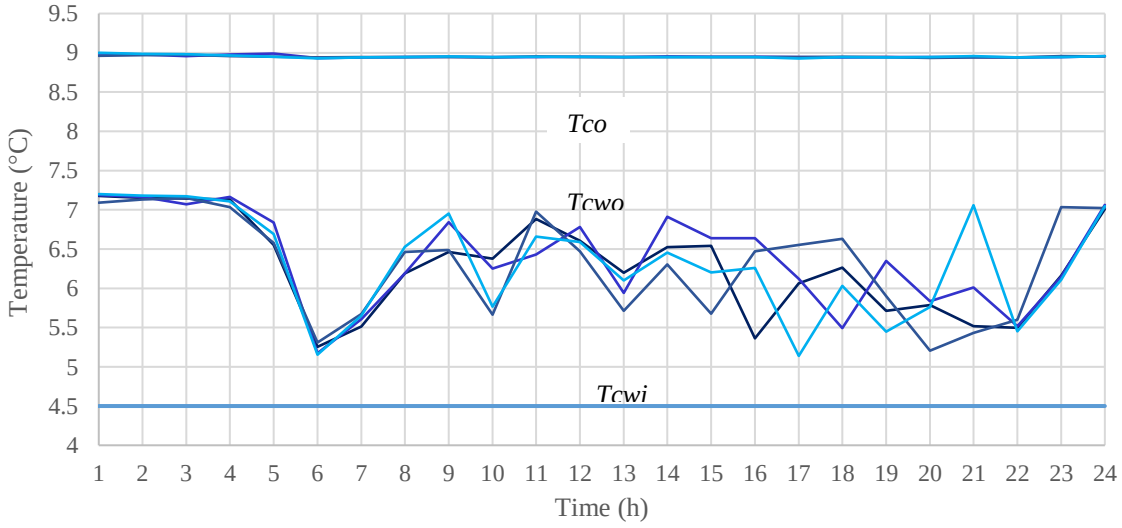

Figure 23. Cold seawater inlet and outlet temperature and condenser temperature

Finally, **Fig.24** and **Fig. 25** show the operational policy of the system in terms of exergetic efficiency and work in the turbine respect to the time.

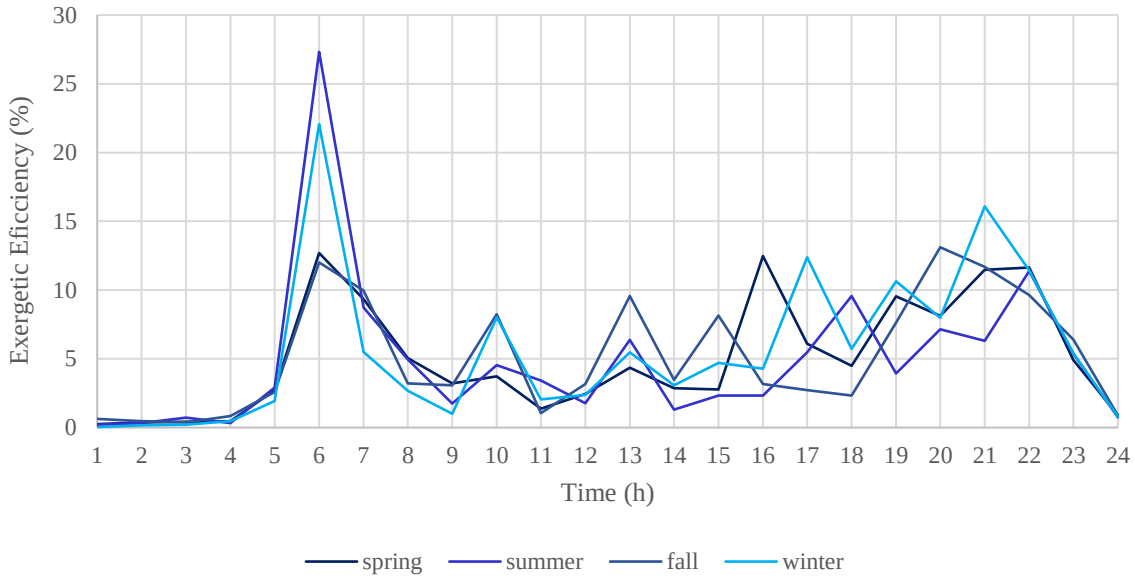

Figure 24. Exergy efficiency

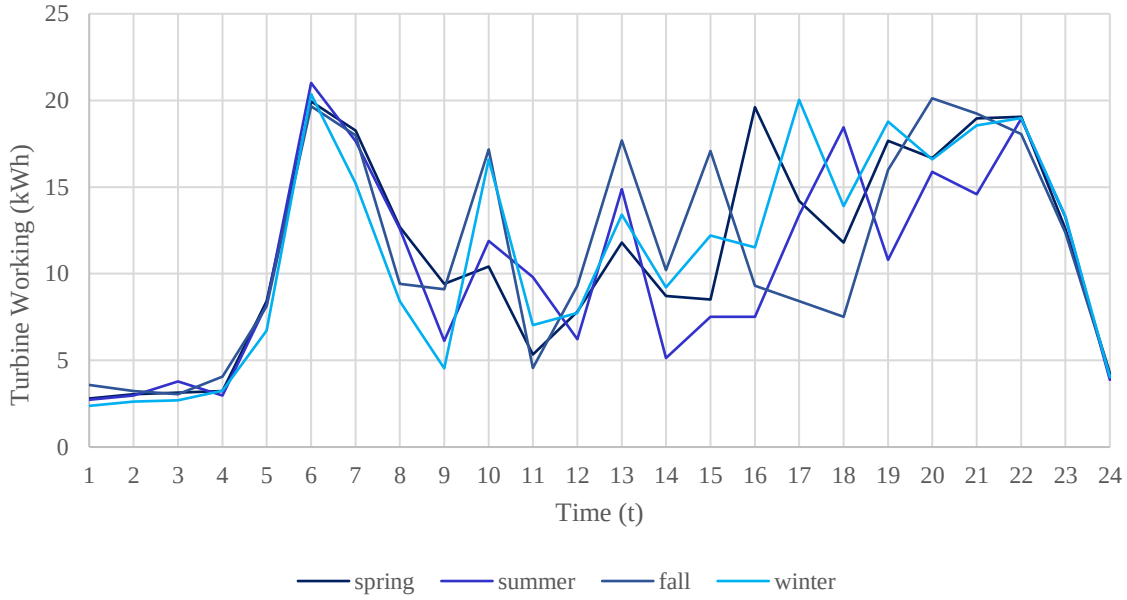

Figure 25. Turbine working

9. Conclusions

A NLP multi-objective multi-period and multi-scenario optimization model has been proposed to design the closed-cycle OTEC plant. The formulation allows selecting the optimal configuration of the system as well as getting the operation policy and sizing of the OTEC plant. The model includes thermodynamic, economic, exergetic aspects as well as the addition of a solar collector in order to improve the efficiency of the system. In addition, the model considers the nonlinear behavior associated with the design and operation of the equipment.

The results show that integrating a solar collector to increase the seawater temperature before entering the evaporator considerably increases the efficiency of the cycle. On the other hand, the TAC is directly associated with the efficiency of the system, therefore the greater the efficiency of the system the greater TAC. This is turn is associated with the solar collector size and hence the TAC of the OTEC plant. On the other way, the areas of the equipment are small compared to other published studies; this is because the approach is multi-period, and that is to say, the system is designed based on the largest requirement of electricity consumed in 1 hour.

Results show the trade-offs between the considered objectives. The configurations represented by each of the points of the Pareto front represent solutions that can be considered in a decision-making framework according to the priorities considered. However, in this paper, a compromise solution based on utopia point is select to present a final solution that involves under equality conditions both objectives.

For future work, it is important to take into account a stochastic focus considering the possible variations in the decision variables that directly affect the performance and design of the system. In the same way, it is important to consider the environmental impact analysis involving in the extraction of seawater, the implementation of the system and the emissions of greenhouse gases emitted. In addition to considering the advantage of the other OTEC, power cycles to produce desalinated water and electricity simultaneously.

References

Ahmad, A., Al-Dadah, R., & Mahmoud, S. (2017). Liquid air utilization in air conditioning and power generating in a commercial building. Journal of Cleaner Production, 149, 773-783.

Ahmadi, P., Dincer, I., & Rosen, M. A. (2015). Multi-objective optimization of an ocean thermal energy conversion system for hydrogen production. *International Journal of Hydrogen Energy*, *40*(24), 7601-7608.

Aydin, H., Lee, H. S., Kim, H. J., Shin, S. K., & Park, K. (2014). Off-design performance analysis of a closed-cycle ocean thermal energy conversion system with solar thermal preheating and superheating. *Renewable energy*, *72*, 154-163.

Block, T., & Paredis, E. (2013). Urban development projects catalyst for sustainable transformations: The need for entrepreneurial political leadership. Journal of Cleaner Production, 50, 181-188.

Bakirtas, T., & Akpolat, A. G. (2018). The relationship between energy consumption, urbanization, and economic growth in new emerging-market countries. *Energy*, *147*, 110-121.

Brooke A, Kendrick D, Meeruas A, Raman R (2014) GAMS-Language guide. GAMS Development Corp, Washington, DC.

Cancino-Solórzano, Y., Villicaña-Ortiz, E., Gutiérrez-Trashorras, A. J., & Xiberta-Bernat, J. (2010). Electricity sector in Mexico: Current status. Contribution of renewable energy sources. *Renewable and Sustainable Energy Reviews*, *14*(1), 454-461.

Cao, Y., Fuentes-Cortes, L. F., Chen, S., & Zavala, V. M. (2017). Scalable modeling and solution of stochastic multiobjective optimization problems. Computers & Chemical Engineering, 99, 185-197.

Cardona, E., & Piacentino, A. (2006). A new approach to exergoeconomic analysis and design of variable demand energy systems. *Energy*, 31(4), 490-515.

Collins, S., Deane, J. P., Poncelet, K., Panos, E., Pietzcker, R. C., Delarue, E., & Gallachóir, B. P. Ó. (2017). Integrating short term variations of the power system into integrated energy system models: A methodological review. *Renewable and Sustainable Energy Reviews*, 76, 839-856.

D'Alisa, G., & Kallis, G. (2016). A political ecology of maladaptation: Insights from a Gramscian theory of the State. Global Environmental Change, 38, 230-242.

Daniel, T. (1985). Aquaculture using cold OTEC water. In *OCEANS'85-Ocean Engineering and the Environment*, 1284-1289. IEEE

Devis-Morales, A., Montoya-Sánchez, R. A., Osorio, A. F., & Otero-Díaz, L. J. (2014). Ocean thermal energy resources in Colombia. *Renewable Energy*, *66*, 759-769.

Diwekar U., David A. (2015) BONUS Algorithm for Large Scale Stochastic Nonlinear Programming Problems. Springer.

Dowling, A. W., Ruiz-Mercado, G., & Zavala, V. M. (2016). A framework for multi-stakeholder decision-making and conflict resolution. Computers & Chemical Engineering, 90, 136-150.

El-Halwagi MM (2017) A return on investment metric for incorporating sustainability in process integration and improvement projects. Clean Technology and Environ Policy 19(2):611–617

Elsafty, A. F., & Saeid, L. A. (2009). Seawater air conditioning [SWAC]: A cost effective alternative. International Journal of Engineering (IJE), 3(3), 346.

Esteban, M., & Leary, D. (2012). Current developments and future prospects of offshore wind and ocean energy. *Applied Energy*, *90*(1), 128-136.

Faizal, M., & Ahmed, M. R. (2013). Experimental studies on a closed cycle demonstration OTEC plant working on small temperature difference. *Renewable energy*, *51*, 234-240.

Fard, R. N., & Tedeschi, E. (2018). Integration of distributed energy resources into offshore and subsea grids. *CPSS Transactions on Power Electronics and Applications*, 3(1), 36-45.

Farnsworth, K. (2010). Business power, social policy preferences and development. In Business, politics and public policy, 63-89.

Freeman, J., Hellgardt, K., & Markides, C. N. (2017). Working fluid selection and electrical performance optimisation of a domestic solar-ORC combined heat and power system for year-round operation in the UK. *Applied Energy*, 186, 291-303.

Fuentes-Cortés, L. F., Ponce-Ortega, J. M., & Zavala, V. M. (2018). Balancing stakeholder priorities in the operation of combined heat and power systems. Applied Thermal Engineering, 128, 480-488.

Ghodsi, S. H., Kerachian, R., Estalaki, S. M., Nikoo, M. R., & Zahmatkesh, Z. (2016). Developing a stochastic conflict resolution model for urban runoff quality management: application of info-gap and bargaining theories. Journal of hydrology, 533, 200-212.

Gong, J., Gao, T., & Li, G. (2013). Performance analysis of 15 kW closed cycle ocean thermal energy conversion system with different working fluids. *Journal of solar energy engineering*, *135*(2), 024501.

González-Bravo, R., Fuentes-Cortés, L. F., & Ponce-Ortega, J. M. (2017). Defining priorities in the design of power and water distribution networks. Energy, 137, 1026-1040.

González-López, R., & Giampietro, M. (2018). Relational analysis of the oil and gas sector of Mexico: Implications for Mexico's energy reform. *Energy*, *154*, 403-414

Hall, N., Lacey, J., Carr-Cornish, S., & Dowd, A. M. (2015). Social licence to operate: understanding how a concept has been translated into practice in energy industries. Journal of Cleaner Production, 86, 301-310.

Hernández-Escobedo, Q., Perea-Moreno, A. J., & Manzano-Agugliaro, F. (2018). Wind energy research in Mexico. *Renewable Energy*, *123*, 719-729.

Hernández-Romero, I. M., Fuentes-Cortés, L. F., & Nápoles-Rivera, F. (2019a). Conditions accommodating a dominant stakeholder in the design of renewable air conditioning systems for tourism complexes. *Energy*, 172,808-822.

Hernández-Romero, I. M., Fuentes-Cortés, L. F., Mukherjee, R., El-Halwagi, M. M., Serna-González, M., & Nápoles-Rivera, F. (2019b). Multi-scenario model for optimal design of seawater air-conditioning systems under demand uncertainty. *Journal of Cleaner Production*, 117863.

Hjaila, K., Puigjaner, L., Laínez, J. M., & Espuña, A. (2017). Integrated game-theory modelling for multi enterprise-wide coordination and collaboration under uncertain competitive environment. Computers & Chemical Engineering, 98, 209-235.

Huesca-Perez, M. E., Sheinbaum-Pardo, C., & Köppel, J. (2016). Social implications of siting wind energy in a disadvantaged region–The case of the Isthmus of Tehuantepec, Mexico. Renewable and Sustainable Energy Reviews, 58, 952-965.

Hiriart, G., & Gutiérrez-Negrín, L. C. (2003). Main aspects of geothermal energy in Mexico. *Geothermics*, *32*(4-6), 389-396

Jorgenson, D. W. (2016). Econometric general equilibrium modeling. Journal of Policy Modeling, 38(3), 436-447.

Jung, J. Y., Lee, H. S., Kim, H. J., Yoo, Y., Choi, W. Y., & Kwak, H. Y. (2016). Thermoeconomic analysis of an ocean thermal energy conversion plant. *Renewable energy*, *86*, 1086-1094.

Khan, N., Kalair, A., Abas, N., & Haider, A. (2017). Review of ocean tidal, wave and thermal Khan energy technologies. *Renewable and Sustainable Energy Reviews*, 72, 590–604

Khennich, M., & Galanis, N. (2012). Optimal design of ORC systems with a low-temperature heat source. *Entropy*, *14*(2), 370-389.

Kim, A. S., Kim, H. J., Lee, H. S., & Cha, S. (2016). Dual-use open cycle ocean thermal energy conversion (OC-OTEC) using multiple condensers for adjustable power generation and seawater desalination. *Renewable energy*, *85*, 344-358.

Kotas, T. J. (1980). Exergy concepts for thermal plant: First of two papers on exergy techniques in thermal plant analysis. *International Journal of Heat and Fluid Flow*, *2*(3), 105-114.

Lilley, J., Konan, D. E., & Lerner, D. T. (2015). Cool as a (sea) cucumber? Exploring public attitudes toward seawater air conditioning in Hawai 'i. Energy Research & Social Science, 8, 173-183.

Liu, W. H., Hashim, H., Lim, J. S., Ho, C. S., Klemeš, J. J., Zamhuri, M. I., & Ho, W. S. (2018). Techno-economic assessment of different cooling systems for office buildings in tropical large city considering on-site biogas utilization. Journal of Cleaner Production, 184, 774-787.

Lozano, M. A., & Valero, A. (1993). Theory of the exergetic cost. *Energy*, 18(9), 939-960.

Marler, R. T., & Arora, J. S. (2004). Survey of multi-objective optimization methods for engineering. *Structural and multidisciplinary optimization*, *26*(6), 369-395.

Mundo-Hernández, J., de Celis Alonso, B., Hernández-Álvarez, J., & de Celis-Carrillo, B. (2014). An overview of solar photovoltaic energy in Mexico and Germany. *Renewable and sustainable energy reviews*, *31*, 639-649.

Mukherjee, R., Sengupta, D., & Sikdar, S. K. (2013). Parsimonious use of indicators for evaluating sustainability systems with multivariate statistical analyses. Clean Technologies and Environmental Policy, 15(4), 699-706.

NCEI (2013) National Centers for Environmental Information. https://data.nodc.noaa.gov/las/UI.vm#panelHeaderHidden. Accessed March 2019

Nihous, G. C. (2007). A preliminary assessment of ocean thermal energy conversion resources. *Journal of Energy Resources Technology*, *129*(1), 10-17.

Nithesh, K. G., & Chatterjee, D. (2016). Numerical prediction of the performance of radial inflow turbine designed for ocean thermal energy conversion system. *Applied energy*, *167*, 1-16.

Pérez-Denicia, E., Fernández-Luqueño, F., Vilariño-Ayala, D., Montaño-Zetina, L. M., & Maldonado-López, L. A. (2017). Renewable energy sources for electricity generation in Mexico: A review. *Renewable and Sustainable Energy Reviews*, 78, 597-613.

Pischke, E. C., Solomon, B., Wellstead, A., Acevedo, A., Eastmond, A., De Oliveira, F., & Lucon, O. (2019). From Kyoto to Paris: Measuring renewable energy policy regimes in Argentina, Brazil, Canada, Mexico and the United States. *Energy Research & Social Science*, 50, 82-91.

Rau, G. H., & Baird, J. R. (2018). Negative-CO2-emissions ocean thermal energy conversion. *Renewable and Sustainable Energy Reviews*, *95*, 265-272.

Rosen, M. A., & Dincer, I. (2004). Effect of varying dead-state properties on energy and exergy analyses of thermal systems. *International Journal of Thermal Sciences*, *43*(2), 121-133.

SENER. Secretariat of Energy. 2017. http://www.gob.mx/sener. [Accessed Mar 2019].

Sun, F., Ikegami, Y., Jia, B., & Arima, H. (2012). Optimization design and exergy analysis of organic rankine cycle in ocean thermal energy conversion. *Applied Ocean Research*, *35*, 38-46.

Sauret, E., & Rowlands, A. S. (2011). Candidate radial-inflow turbines and high-density working fluids for geothermal power systems. *Energy*, *36*(7), 4460-4467.

Tauro, R., García, C. A., Skutsch, M., & Masera, O. (2018). The potential for sustainable biomass pellets in Mexico: An analysis of energy potential, logistic costs and market demand. *Renewable and Sustainable Energy Reviews*, *82*, 380-389.

Tian, Y., & Zhao, C. Y. (2013). A review of solar collectors and thermal energy storage in solar thermal applications. *Applied energy*, *104*, 538-553.

Trier D. Solar collectors. In: Solar district heating guidelines – collection of fact sheets. Solar district heating – intelligent energy – Europe; 2012. p. 1–15.

Vidal-Amaro, J. J., Østergaard, P. A., & Sheinbaum-Pardo, C. (2015). Optimal energy mix for transitioning from fossil fuels to renewable energy sources–The case of the Mexican electricity system. *Applied Energy*, *150*, 80-96.

Von Herzen, B., Theuretzbacher, T., Newman, J., Webber, M., Zhu, C., Katz, J. S., & Ramaswamy, M. (2017). A Feasibility Study of an Integrated Air Conditioning, Desalination and Marine Permaculture System in Oman. In *ICTEA: International Conference on Thermal Engineering*.

Wang, J. C. (2012). A study on the energy performance of hotel buildings in Taiwan. Energy and Buildings, 49, 268-275.

War, J. C. (2011). Seawater Air Conditioning (SWAC) a renewable energy alternative. In OCEANS 2011 (pp. 1-9). IEEE.

Whitton, J., Parry, I. M., Akiyoshi, M., & Lawless, W. (2015). Conceptualizing a social sustainability framework for energy infrastructure decisions. Energy Research & Social Science, 8, 127-138.

Wu, J., Liu, C., Li, H., Ouyang, D., Cheng, J., Wang, Y., & You, S. (2017). Residential air-conditioner usage in China and efficiency standardization. Energy, 119, 1036-1046.

Yamada, N., Hoshi, A., & Ikegami, Y. (2009). Performance simulation of solar-boosted ocean thermal energy conversion plant. *Renewable Energy*, *34*(7), 1752-1758.

Yamada, N., Hoshi, A., & Ikegami, Y. (2006). Thermal efficiency enhancement of ocean thermal energy conversion (OTEC) using solar thermal energy. In *4th International Energy Conversion Engineering Conference and Exhibit (IECEC)* (p. 4130).

Yang, M. H., & Yeh, R. H. (2014). Analysis of optimization in an OTEC plant using organic Rankine cycle. *Renewable Energy*, 68, 25-34.

Zárate-Toledo, E., Patiño, R., & Fraga, J. (2019). Justice, social exclusion and indigenous opposition: A case study of wind energy development on the Isthmus of Tehuantepec, Mexico. *Energy Research & Social Science*, 54, 1-11.

Zhang, M. M., Wang, Q., Zhou, D., & Ding, H. (2019). Evaluating uncertain investment decisions in low-carbon transition toward renewable energy. *Applied Energy*.

ANEXO I GAMS CODE

```
*Closed-cylce Optimization Gams version written by
*Ilse M. / January, 2019
*UNIVERSIDAD MICHOACANA

$TITLE CLOSED CYCLE
OPTION mip=cplex;
OPTION MINLP =dicopt;
OPTION NLP=baron;
option optca=.001;
option optcr=.001;
Option reslim=9E9;

SETS
s season in the year /spring,summer,fall,winter/
t period time in hours /1*24/;

Parameters
RHOSW    DENSIDAD AGUA DE MAR (kg per m^3) /1026.562/
cpsw     CP DEL AGUA (kWh per Kg°C) /0.001109/
KF       FACTOR USED TO ANNUALIZE THE CAPITAL COSTS(YEAR-1) /0.463/
TAM      AMBIENT TEMPERATURE IN (°C) /24/
nof      OPTICAL EFFICIENCY /0.8/
CKWH     ELECTRICITY UNITARY COST $ 0.978 MX ($US PER kWh) /0.052/
;

TABLE ELCON(t,s) ELECTRICITY CONSUMPTION kWh
          spring     summer     fall       winter
1         0.6        0.5        1.5        0.1
2         0.9        0.8        1.1        0.4
3         1          1.7        0.9        0.5
4         1.1        0.8        2          1.1
5         6.4        6.2        6.1        4.6
6         18.2       21         17.8       18.8
7         16.3       15.7       16         13.1
8         10.7       10.6       7.4        6.3
9         7.4        4.1        7.1        2.4
10        8.4        9.9        15.2       14.5
11        3.3        7.8        2.5        4.9
12        5.8        4.2        7.3        5.6
13        9.8        12.9       15.7       11.3
14        6.7        3.1        8.2        7.1
15        6.5        5.5        15.1       10.1
16        17.7       5.5        7.3        9.4
17        12.2       11.4       6.4        18.1
18        9.8        16.5       5.5        11.8
19        15.7       8.8        14         16.7
20        14.7       13.9       18.7       14.5
21        17         12.6       17.3       16.4
22        17.1       17         16.1       16.9
23        10.6       11.3       10.3       11.2
24        2.2        1.8        2.1        1.9
```

```
 58 TABLE Eg(t,s) kWh PER M^2 PER HOUR
 59           spring      summer        fall       winter
 60 1         0.00         0.00        0.00        0.00
 61 2         0.00         0.00        0.00        0.00
 62 3         0.00         0.00        0.00        0.00
 63 4         0.00         0.00        0.00        0.00
 64 5         0.00         0.00        0.00        0.00
 65 6         0.02         0.02        0.01        0.01
 66 7         0.05         0.06        0.03        0.03
 67 8         0.14         0.14        0.09        0.07
 68 9         0.24         0.27        0.16        0.17
 69 10        0.44         0.53        0.38        0.33
 70 11        0.68         0.66        0.47        0.47
 71 12        0.82         0.88        0.61        0.72
 72 13        0.92         0.96        0.80        0.73
 73 14        0.85         0.85        0.68        0.69
 74 15        0.61         0.71        0.56        0.53
 75 16        0.44         0.47        0.36        0.30
 76 17        0.21         0.25        0.19        0.16
 77 18        0.13         0.11        0.08        0.07
 78 19        0.05         0.06        0.03        0.02
 79 20        0.01         0.02        0.01        0.01
 80 21        0.00         0.00        0.00        0.00
 81 22        0.00         0.00        0.00        0.00
 82 23        0.00         0.00        0.00        0.00
 83 24        0.00         0.00        0.00        0.00
 84 ;
 85
 86 Parameter TWSI(s)  SEAWATER INLET TEMPERATURE IN °C
 87 /spring     29.58
 88  summer     29.87
 89  fall       29.52
 90  winter     28.42/;
 91
 92 Parameter TM(s)  MEAN TEMPERATURE  IN °C;
 93 TM(s)=(TWSI(s)+30)/2;
 94
 95 Parameter Dt1(s) TEMPERATURE DIFERENTIAL;
 96 Dt1(s)=TM(s)-TAM;
 97
 98 Parameter
 99 ncs(s) SOLAR COLECTOR EFICIENCY;
100 *ncs(t,s)=nof-((k1*Dt1(s))/Eg(t,s))-((k2*Dt1(s)**2)/Eg(t,s));
101 ncs(s)=-0.000006796*(Dt1(s)**2)-0.00325*Dt1(s)+nof;
102
103
104
105 POSITIVE VARIABLES
106 QSC(t,s)          ENERGY BALANCE IN SOLAR COLECTOR(kWh)
107 ASC               SOLAR COLLECTOR AREA (m^2)
108 mwsin(t,s)       AMOUNT OF SEAWATER THAT US AT THE INLET OF THE SOLAR COLLECRTOR»
     (kg)
109 msc(t,s)          AMOUNT OF SEAWATER THAT US AT THE OUTLET OF THE SOLAR COLLECRTO»
    R (kg)
110 TSCO(t,s)         OUTPUT TEMPERATURE FROM SOLAR COLECTOR(°C)
```

```
115 EQUATIONS
116 C1
117 C2
118 C3;
119 *C5;
120
121 C1(t,s)..             mwsin(t,s)=E=msc(t,s);
122 C2(t,s)..             QSC(t,s)=E=Eg(t,s)*ncs(s)*ASC;
123 C3(t,s)..             mwsin(t,s)*cpsw*TWSI(s)+QSC(t,s)=E=msc(t,s)*cpsw*TSCO(t,s);
124 *C5(t,s)..             TSCO(t,s)=L=60;
125
126 mwsin.l(t,s)=100;
127 ********************************SOLAR COLLECTOR COST*************************»
    *****************
128 PARAMETERS
129 FCSC     FIXED COST FOR SOLAR COLLECTOR /30/
130 VCSC     VARIABLE COST FOR SOLAR COLLECTOR  /30/
131 *ALPHA    EXPONENT FOR SOLAR COLLECTOR AREA COST /1/
132 OMSC     O&M COST ($ PER kWh)/0.0005/
133 HD       OPERATION (DAYS) /91.25/;
134
135 POSITIVE VARIABLES
136 SCCOST   SOLAR COLLECTOR COST ($)
137 mwsmax   MAX MASS INTERING IN ALL TIMES (kg)
138 OMCOST   OPERATIONAL ANDMAINTENANCE COST FOR SOLAR COLLECTOR ($);
139
140 EQUATIONS
141 SC1,
142 *WR1,
143 OM1;
144
145 SC1..               SCCOST=E=(FCSC+(VCSC*(ASC)));
146
147
148 ASC.up=500;
149
150 ********************************OPERATION AND MAINTENANCE COST FOR SOLAR COLLE»
    CTOR ***************
151
152 OM1..     OMCOST=E=OMSC*HD*(sum(s,sum(t,QSC(t,s))));
153
154 ***************************************************************************EVAPORATOR**»
```

```
QEV(t,s)              Q EVAPORATOR(kWh)
AEV                   EVAPORATOR AREA (m^2)
QEVMAX                Q MAX EVAPORATOR(kWh)
DTEVMAX
NNET(t,s)             NET EFFICIENCY
DTMLEV(T,S)           DIFERENTIAL T IN EVAPORATOR IN (°C)
TEV(T,S)              EVAPORATOR TEMPERATURE
TWSO(T,S)             OUTPUT SEAWATER FLOW OF THE HEAT EXCH(kg)
mwf
P_2(t,s)
P_3(t,s)
h3(t,s)
S3(t,s)
h2(t,s)
T_2(t,s)
DTI1(t,s),DTI2(t,s),DTI3(t,s);



EQUATION
e1,e2,e3,e4,e5,e6,e7,E8,e9,e11,e12,e13,e14,e15,e1a,e2a;
*e1,e2,e3,e7,e11,e12,e13,e14,e15;


e1(t,s)..               msc(t,s)=E=mwev(t,s);

e2(t,s)..               QEV(t,s)=E=mwf*nev*(h3(t,s)-h2(t,s));

e3(t,s)..               QEV(t,s)=E=mwev(t,s)*cpsw*(TSCO(t,s)-TWSO(T,S));

e4(t,s)..               TWSO(T,S)-TEV(t,s)=G=3;

e5(t,s)..               DTI1(t,s)=E=TSCO(t,s)-TEV(t,s);
e6(t,s)..               DTI2(t,s)=E=TWSO(t,s)-TEV(t,s);
e7(t,s)..               DTI3(t,s)=E=TSCO(t,s)-TWSO(t,s);

e8(t,s)..               DTMLEV(t,s)*(log(DTI1(t,s)/DTI2(t,s)))=E=DTI3(t,s);

e1a(t,s)..              QEVMAX=G=QEV(t,s);

e2a(t,s)..              DTEVMAX=G=DTMLEV(t,s);

e9(t,s)..               AEV*UEV*DTEVMAX=E=QEVMAX;

e11(t,s)..              h3(t,s)=E=(382.1+1.106*TSCO(t,s)-10.09*P_3(t,s))*f1;

e16(t,s)..              S3(t,s)=e=1.713+0.002645*TSCO(t,s)-0.08441*P_3(t,s);

e12(t,s)..              h2(t,s)=E=(1.597*T_2(t,s)+194.9)*f1;
```

```
PR2(t,s)..      WP(t,s)=E=((h2(t,s)-h1(t,s))*mwf)/(NWFP*NWM);

PR3(t,s)..      WPMAX=G=WP(t,s);

*T_1.fx(t,s)=17;


*************************************************************************RELACION ENT»
ALPIA-PRESION*****
PR4(t,s)..      PRE1(t,s)=E=(0.000318*T_1(t,s)**2+0.003424*T_1(t,s)+0.3513);
PR5(T,S)..      S1(t,s)=e=0.000006*T_1(t,s)**2+0.00431*T_1(t,s)+1.006;
PR6(t,s)..      S2(t,s)=E=S1(t,s);
*PR4(t,s)..      S2(t,s)=e=h1(t,s)+0.0016*(P_2(t,s)-PRE1(t,s));

*****************************************WORKING FLUID PUMP COST*************»
*************
WC1..           WFPCOST=E=3500*(WPMAX)**0.41;



*mwf.up=300;


*************************************************************************TURBINE*****»
**************************************************
PARAMETER
NG        GENERATOR EFFICIENCY /0.9/
NT        TURBINE EFFICIENCY /0.87/;

POSITIVE VARIABLE
h4(t,s)            ENTHALPY 4  (kWh PER kg)
T_4(t,s)           TEMPERATURE 4 (°C)
WT(t,s)              MAXIMUM WORK IN THE TURBINE (kWh)
S4(t,s)
WTMAX;


EQUATION
TR1,
TR2,TR4,TR3,TR5
TR6;

TR1(t,s)..        S4(t,s)=E=S3(t,s);
TR2(t,s)..        T_4(t,s)=L=TSCO(t,s)-3;
TR5(t,s)..        h4(t,s)=E=h1(t,s)+T_4(t,s)*(S4(t,s)-S1(t,s));
*f1;
TR3(t,s)..        h4(t,s)=L=h3(t,s);

TR4(t,s)..        WT(t,s)=E=mwf*(h3(t,s)-h4(t,s))*NG*NT;

*TR5(t,s)..        h4(t,s)=E=(-0.00428*T_4(t,s)**2+0.7329*T_4(t,s)+397.4)*f1 ;
```

```
---
331 ***********************************TURBINE COST*********************************»
    *********
332 PARAMETER
333 BETA    EXPONENT FOR TURBINE COST /0.41/;
334
335 POSITIVE VARIABLES
336 TCOST   TURBINE COST;
337
338 EQUATIONS
339 TU1;
340
341 TU1..   TCOST=E=2237*(WTMAX)**BETA;
342
343 ***************************************************************************CONDENSER***»
    *******************************************
344
345 PARAMETER
346 nco              CONDENSER EFFICIENCY /0.9/
347 UCO              OVERALL HEAT EXCHANGER (kW PER m^2 °C)/0.1358/
348 TCWI       /5/;
349
350
351 POSITIVE VARIABLE
352 mcwi(t,s)          COLD SEAWATER FLOW INLET (kg)
353 mcwo(t,s)          COLD WATER OUTPUT (kg)
354 QCO                Q CONDENSER (kWh)
355 ACO                CONDENSER AREA  (m^2)
356 TCWO(t,s)
357 TCO(t,s)
358 DCI1,DCI2,DCI3
359 DTMLCO(t,s)
360 DTMLCOM,QCOMAX;
361
362
363 EQUATION
364 cc1,
365 cc2,
366 cc3
367 cc4,cc5,cc6,cc7,cc8,
368 *cc9,
369 cc10,cc11,cc12;
370
371
372 cc1(t,s)..              mcwi(t,s)=E=mcwo(t,s);
373
```

```
cc5(t,s)..                DCI1(t,s)=E=TCWO(t,s)-TCWI;
cc6(t,s)..                DCI2(t,s)=E=TCO(t,s)-TCWI;
cc7(t,s)..                DCI3(t,s)=E=TCO(t,s)-TCWO(t,s);

cc8(t,s)..                DTMLCO(t,s)*(log(DCI2(t,s)/DCI3(t,s)))=E=DCI1(t,s);

*cc9(t,s)..                TEV(t,s)-TCO(T,S)=G=0.2;

DCI2.lo(t,s)=0.1;
DCI3.lo(t,s)=0.1;
DCI1.lo(t,s) =0.1;
TCO.up(T,S)=9;
ACO.UP=500;
*ACO.FX=1;

mcwi.l(t,s)=100;

ccl0(t,s)..               QCOMAX=G=QCO(t,s);
ccl1(t,s)..               DTMLCOM=G=DTMLCO(t,s);

ccl2(t,s)..               ACO*UCO*DTMLCOM=E=QCOMAX;


**********************************CONDENSER COST*******************************»
***********

POSITIVE VARIABLES
COCOST   CONDENSER COST;


EQUATIONS
CO1;

CO1..   COCOST=E=150*(ACO)**0.8;


*****************************************************PIPE COST FOR WAR SEAWATER*»
******************
$ontext
PARAMETERS
L    LENGHT OF WARM SEWATER PIPE IN (m) /50/
L1   LENGHT OF COLD SEWATER PIPE IN (m) /900/
Dm   DIAMETER OF WARM SEAWATER PIPE IN (m) /0.3/
Dm1  DIAMETER OF COLD SEAWATER PIPE IN (m) /0.3/
*parametros obtenidos de swamee & sharma y sn para diametros de 0.25m-0.75m
km   COST PARAMETER ACCORDING TO TYPE OF PIPE MATERIAL /480/
mp  EXPONENTE DE COSTO DE ACUERDO TIPO DE MATERIAL TUBERIA /0.935/ ;

POSITIVE VARIABLE
WSPIPE       COST OF WARM SEAWATER PIPING ($)
CSPIPE       COST OF COLD SEAWATER PIPING ($)
PIPINGCOST   PIPNG COST ($)    ;
```

```
440 SEG1..  WSPIPE=E=km*L*(Dm**mp);
441 SG2..   CSPIPE=E=km*L1*(Dm1**mp);
442
443 SEG3..  PIPINGCOST=E=(WSPIPE+CSPIPE);
444 $offtext
445
446 ***************************************************************PUMPS************
447
448 PARAMETERS
449 NWS              COLD AND WARM SEAWATER PUMPS EFFICIENCY /0.85/
450 g                GRAVITY (m PER s^2)/9.8/
451 DCH               TOTAL PRESSURE DIFFERENCE FOR COLD S PUMP(I.E HEAD LOSS) IN m »
    /0.843/
452 DH              TOTAL PRESSURE DIFFERENCE FOR WARM S PUMP(I.E HEAD LOSS) IN m /3»
    /;
453
454 POSITIVE VARIABLES
455 WPCW(t,s)        PUMP WORK (COLD SEAWATER kWh)
456 WPWS(t,s)        PUMP WORK (WARM SEAWATER kWh)
457 wwpsm            MAX SEAWATER IN ALL TIMES
458 wcpsm            MAX SEAWATER IN ALL TIMES;
459
460 EQUATIONS
461 W1,W2,W3,W4;
462 ****************************************COLD WATER PUMP*********************»
    ****************************
463
464 W1(t,s)..            WPCW(t,s)=E=((mcwi(t,s)*g*DH)/NWS)*f1;
465 ***************************************WARM SEAWATER PUMP*********************»
    **********************
466
467 W2(t,s)..            WPWS(t,s)=E=((mwsin(t,s)*g*DCH)/NWS)*f1;
468
469 w3(t,s)..            wcpsm=G=WPCW(t,s);
470
471 w4(t,s)..            wwpsm=G=WPWS(t,s);
472
473 mcwi.l(t,s)=100;
474
475 POSITIVE VARIABLES
476 WSPCOST   WARM SEAWATER PUMP COST
477 WCPCOST   COLD SEAWATER PUMP COST;
478
479 EQUATIONS
480 WP1,WP2;
```

```
Wn(t,s)..          ELCON(t,s)=E=WNET(t,s);
WN2(t,s)..         WNMAX=G=WNET(t,s);

*************************************GENERATOR COST*****************************»
************************
POSITIVE VARIABLES
GCOST   GENERATOR COST;

EQUATIONS
G1,TRN,WR5;

G1..   GCOST=E=176*(WNMAX);

*WNMAX.UP=21;
************************************WORKING FLUID MASS COST*********************»
**********************
PARAMETER
PUWF   WORKING FLUID UNITARY COST  PER KG (180MXN) $ /20/;

POSITIVE VARIABLE
WPCO  WORKING FLUID TOTAL COST;

EQUATION
PW1;

PW1..    WPCO=E=PUWF*mwf;

*******************************************************************************»
*********************************
TRN(t,s)..              WNET(t,s)=E=WT(t,s)-(WP(t,s)+WPWS(t,s)+WPCW(t,s));

WR5(t,s)..              NNET(t,s)*QEV(t,s)=E=WNET(t,s);

*SE1(t,s)..              mwsin(t,s)=G=mcwi(t,s);


$ontext
*****************************************EXERGY ANALYSIS******************
Parameter
ho STD CONDITIONS KJ per kg/104.89/
so STD CONDITIONS kJ per kg k /0.036/  ;

Parameter hws(s) INLET warm TEMPERATURE ENTHALPY KJ per kg;
hws(s)=4.118*TWSI(s)+3.102;

Parameter hcw INLET cold TEMPERATURE ENTHALPY KJ per kg;
hcw=4.118*TCWI+3.102;
```

```
547 POSITIVE VARIABLES
548 hsc,ssc,EXSW,EXSWkwh,EXCW,EXCWkwh,EXSC,EXSCkwh,NEXER;
549
550
551 EQUATIONS
552 ex1,ex2,ex3,ex4,ex5,ex6,ex7,ex8,ex9;
553
554 ex1(t,s)..                hsc(t,s)=E=(4.118*TSCO(t,s)+3.102);
555 ex2(t,s)..                ssc(t,s)=E=(0.01326*TSCO(t,s)+0.003311);
556
557
558 ex3(t,s)..                EXSW(t,s)=E=mwsin(t,s)*((hws(s)-ho)-25*(sws(s)-so));
559 ex4(t,s)..                EXSWkwh(t,s)=E=EXCW(t,s)*0.000277778;
560
561 ex5(t,s)..                EXCW(t,s)=E=mcwi(t,s)*((hcw-ho)-25*(scw-so));
562 ex6(t,s)..                EXCWkwh(t,s)=E=EXCW(t,s)*0.000277778;
563
564 ex7(t,s)..                EXSC(t,s)=E=mwsin(t,s)*((hsc(t,s)-ho)-25*(ssc(t,s)-so)»
    );
565 ex8(t,s)..                EXSCkwh(t,s)=E=EXSC(t,s)*0.000277778;
566
567 ex9(t,s)..                NEXER(t,s)*(EXSCkwh(t,s)+EXCWkwh(t,s)+EXSWkwh(t,s))=E=»
    WNET(t,s);
568
569 NEXER.UP(t,s)=1;
570
571 VARIABLE
572 EXERGYEF
573 TAC;
574
575
576 EQUATION
577 EXEF,
578 OBJECTIVE;
579
580 EXEF..              EXERGYEF=E=(SUM((t,s),NEXER(t,s))/96);
581
582
583 $offtext
584 VARIABLE
585 TAC;
586
587 EQUATION
588 OBJECTIVE;
589
590 OBJECTIVE..          TAC=E=(SCCOST+OMCOST+WFPCOST+GCOST+TCOST+EVCOST+COCOST+WSPCO»
    ST+WCPCOST+WPCO);
591 *FNE..    EFOB=E=SUM(t,sum(s,NNET(t,s)))+TAC*0.00000000001EVCOST;
```

```
164 QEV(t,s)              Q EVAPORATOR(kWh)
165 AEV                   EVAPORATOR AREA (m^2)
166 QEVMAX                Q MAX EVAPORATOR(kWh)
167 DTEVMAX
168 NNET(t,s)             NET EFFICIENCY
169 DTMLEV(T,S)           DIFERENTIAL T IN EVAPORATOR IN (°C)
170 TEV(T,S)              EVAPORATOR TEMPERATURE
171 TWSO(T,S)             OUTPUT SEAWATER FLOW OF THE HEAT EXCH(kg)
172 mwf
173 P_2(t,s)
174 P_3(t,s)
175 h3(t,s)
176 S3(t,s)
177 h2(t,s)
178 T_2(t,s)
179 DTI1(t,s),DTI2(t,s),DTI3(t,s);
180
181
182
183 EQUATION
184 e1,e2,e3,e4,e5,e6,e7,E8,e9,e11,e12,e13,e14,e15,e16,e1a,e2a;
185 *e1,e2,e3,e7,e11,e12,e13,e14,e15;
186
187
188 e1(t,s)..               msc(t,s)=E=mwev(t,s);
189
190 e2(t,s)..               QEV(t,s)=E=mwf*nev*(h3(t,s)-h2(t,s));
191
192 e3(t,s)..               QEV(t,s)=E=mwev(t,s)*cpsw*(TSCO(t,s)-TWSO(T,S));
193
194 e4(t,s)..               TWSO(T,S)-TEV(t,s)=G=3;
195
196 e5(t,s)..               DTI1(t,s)=E=TSCO(t,s)-TEV(t,s);
197 e6(t,s)..               DTI2(t,s)=E=TWSO(t,s)-TEV(t,s);
198 e7(t,s)..               DTI3(t,s)=E=TSCO(t,s)-TWSO(t,s);
199
200 e8(t,s)..               DTMLEV(t,s)*(log(DTI1(t,s)/DTI2(t,s)))=E=DTI3(t,s);
201
202 e1a(t,s)..              QEVMAX=G=QEV(t,s);
203
204 e2a(t,s)..              DTEVMAX=G=DTMLEV(t,s);
205
206 e9(t,s)..               AEV*UEV*DTEVMAX=E=QEVMAX;
207
208 e11(t,s)..              h3(t,s)=E=(382.1+1.106*TSCO(t,s)-10.09*P_3(t,s))*f1;
209
210 e16(t,s)..              S3(t,s)=e=1.713+0.002645*TSCO(t,s)-0.08441*P_3(t,s);
211
212 e12(t,s)..              h2(t,s)=E=(1.597*T_2(t,s)+194.9)*f1;
```

```
224 TEV.LO(T,S)=20;
225 TWSO.LO(T,S)=15;
226 *TSCO.LO(t,s)=30;
227 AEV.LO=5;
228 AEV.UP=500;
229 mwf.l=10;
230 *mwf.up=500;
231 DTI2.lo(t,s)=1.5;
232 DTI1.lo(t,s)=1.5;
233 *DTMLEV.UP(t,s)=10;
234
235 *P_3.lo(t,s)=1;
236
237 ***********************************EVAPORATOR COST*******************************»
    ******************************
238
239 POSITIVE VARIABLES
240 EVCOST   EVAPORATOR COST ($)
241
242 EQUATIONS
243 EV1;
244
245 EV1..   EVCOST=E=276*(AEV)**0.88;
246
247
248
249 ***************************************************************************WORKING FLUI»
    D PUMP***********************************************
250 PARAMETER
251 NWFP         WORK FLUID PUMP EFFICIENCY /0.85/
252 NWM          MOTOR EFFICIENCY /0.9/
253 ;
254
255 POSITIVE VARIABLE
256 WP(t,s)              PUMP WORK (kWh)
257 mwf                  WORKING FLUID MASS (kg)
258 hl(t,s)              ENTHALPY 1(kWh PER Kg)
259 T_1(t,s)             CONDENSATION TEMPERATURE (°C)
260 PRE1(t,s)            PRESSURE IN POINT 1
261 WPMAX                MAX WORK IN WFP (kWh)
262 S2(t,s)
263 S1(t,s)
264 WFPCOST              WORKING FLUID PUMP COST ($);
265 *WFPO(t,s)            WORKING FLUID PUMP POWER (kW);
266
267 EQUATION
268 PR1,PR2,
269 PR3,
270 PR4,PR5,PR6,
271 WC1;
272 *PR7;
273
274 PR1(t,s)..      hl(t,s)=E=(1.597*T_1(t,s)+194.9)*f1;
```

ANEXO II PUBLICATIONS

Clean Technologies and Environmental Policy (2018) 20:639–654
https://doi.org/10.1007/s10098-018-1493-7

ORIGINAL PAPER

Optimal design of air-conditioning systems using deep seawater

Ilse María Hernández-Romero[1] · Fabricio Nápoles-Rivera[1] · Rajib Mukherjee[2] · Medardo Serna-González[1] · Mahmoud M. El-Halwagi[3,4]

Received: 5 October 2017 / Accepted: 16 January 2018 / Published online: 27 January 2018

Abstract
This paper presents a multi-objective mixed integer linear programming problem for the optimization of seawater air-conditioning systems using deep seawater as a cooling utility. The optimization formulation was developed including the technical, economic and environmental aspects of the problem. The model is used to define the optimal scheduling of deep seawater use and electricity needed to satisfy the air-conditioning requirements in a group of hotels. It also addresses the optimal planning for biocide, neutralization chemical dosing and mechanical maintenance required to maintain optimal operation conditions in the system. The proposed model is applied to a case study in Mexico. Results show the trade-offs between economic and environmental aspects. Optimal solutions compensating economic and environmental objectives are identified through a Pareto front.

Keywords Seawater air-conditioning (SWAC) · Greenhouse gas emission (GHGE) · Multi-objective optimization · Energy consumption · Mixed integer linear programming (MILP)

https://doi.org/10.1007/s10098-018-1493-7

Hernández-Romero, I. M., Fuentes-Cortés, L. F., & Nápoles-Rivera, F. (2019). Conditions accommodating a dominant stakeholder in the design of renewable air conditioning systems for tourism complexes. *Energy*, 172,808-822.

Energy 172 (2019) 808–822

Contents lists available at ScienceDirect

Energy

journal homepage: www.elsevier.com/locate/energy

Conditions accommodating a dominant stakeholder in the design of renewable air conditioning systems for tourism complexes

Ilse María Hernández-Romero [a], Luis Fabián Fuentes-Cortés [b, *], Fabricio Nápoles-Rivera [a]

[a] Chemical Engineering Department, Universidad Michoacana de San Nicolás de Hidalgo, Morelia, Michoacán, 58060, Mexico
[b] Tecnologico de Monterrey, Escuela de Ingeniería y Ciencias, Ave. Eugenio Garza Sada 2501, Monterrey, NL, 64849, Mexico

ARTICLE INFO

Article history:
Received 8 June 2018
Received in revised form
24 January 2019
Accepted 3 February 2019
Available online 4 February 2019

Keywords:
Dominant stakeholder
Multi-objective design
Seawater air conditioning systems
Renewable energy
Multi-criteria decision-making framework

ABSTRACT

Seawater air conditioning systems use cold water from the deep ocean to provide cooling utilities to buildings. Their design, as with other renewable energy systems, involves the participation of multiple stakeholders with different preferences and objectives. A multi-objective strategy based on compromise solutions for reducing the dissatisfaction between multiple participants is presented. The dominant stakeholder is considered to have predominant participation, opinion, and weight in the final decision of the project. The presented decision-making framework allows for the resolution of conflicts and shows the effects of different criteria on the final configuration of the system. This work presents an optimal design model considering, as a case study, a touristic zone in Mexico. The results show significant differences between scenarios where all the stakeholders are considered under a condition of equality and one in which only the dominant stakeholder is considered. This decision-making approach shows flexibility and provides tolerance limits for compromise solutions that still consider the influence of the dominant stakeholder.

https://doi.org/10.1016/j.energy.2019.02.019

Highlights

- A multi-objective model for design of seawater air conditioning system is presented.
- A multi-stakeholder framework for defining priorities in energy design is used.
- The concept of dominant stakeholder is introduced.
- Compromise solutions reduce the dissatisfaction of stakeholders.
- Flexibility about compromise solution for dominant stakeholders is addressed.

Journal of Cleaner Production 238 (2019) 117863

Contents lists available at ScienceDirect

Journal of Cleaner Production

journal homepage: www.elsevier.com/locate/jclepro

Multi-scenario model for optimal design of seawater air-conditioning systems under demand uncertainty

Ilse María Hernández-Romero [a], Luis Fabián Fuentes-Cortés [b], Rajib Mukherjee [c], Mahmoud M. El-Halwagi [c, d], Medardo Serna-González [a], Fabricio Nápoles-Rivera [a, *]

[a] Chemical Engineering Department, Universidad Michoacana de San Nicolás de Hidalgo, Morelia, Michoacán, 58060, Mexico
[b] Tecnológico Nacional de México, Instituto Tecnológico de Celaya, Departamento de Ingeniería Química, Celaya, Guanajuato, 38010, Mexico
[c] Gas and Fuels Research Center, Texas A&M Engineering Experiment Station, College Station, TX, 77843, United States
[d] Artie McFerrin Department of Chemical Engineering, Texas A&M University, College Sation, TX, 77843, United States

ARTICLE INFO

Article history:
Received 12 October 2018
Received in revised form
29 July 2019
Accepted 31 July 2019
Available online 3 August 2019

Handling Editor. Prof. Jiri Jaromir Klemeš

Keywords:
Optimization under uncertainty
Multi-objective optimization
Seawater air-conditioning (SWAC)
Kernel density estimator (KDE)

ABSTRACT

Seawater air conditioning (SWAC) systems use deep seawater as a cooling utility.

SWAC systems are receiving increasing attention as an integral component of sustainable cooling units of lodging complexes because of the availability of seawater, the substitution of chemicals refrigerants, low achievable temperature, low environmental impact, and large potential savings in energy consumption compared to conventional air-conditioning systems. The design of these systems depends mainly on the energy demand of each hotel in each month; however, there is uncertainty in this variable, since it depends on the season of the year, being lower in months of low occupancy and higher in months of high tourist occupancy. This paper presents a multi-objective optimization with a probabilistic formulation approach for designing these systems under seasonal energy demand uncertainty. The model seeks to meet the demands of air conditioning in hotels using deep seawater considering technical aspects and seeks to minimize the total annual cost while minimizing emissions of greenhouse gases. The results show the importance of accounting uncertainty in the design of these systems.

https://doi.org/10.1016/j.jclepro.2019.117863

Highlights

- A multi-objective multi-scenario stochastic model for the optimal design of SWAC networks is presented
- SWAC systems are an environmentally friendly alternative to conventional AC systems
- The flexibility in the operation of the system can compensate the uncertainty in the energy demand

Hernández-Romero, I. M., Fuentes-Cortés, L. F., Mukherjee, R., El-Halwagi, M. M., Serna-González, M., & Nápoles-Rivera, F. (2019). Multi-scenario model for optimal design of seawater air-conditioning systems under demand uncertainty. *Journal of Cleaner Production*, 117863.

Available online at www.sciencedirect.com

ScienceDirect

IFAC PapersOnLine 52-2 (2019) 207–211

IFAC Papers Online
CONFERENCE PAPER ARCHIVE

Optimal configuration of metallic nanoparticles to maximize heat transfer in a 2D square plate

Ilse María Hernández-Romero*, Antonio Flores-Tlacuahuac, Luis Fabián Fuentes-Cortés***, Fabricio Nápoles-Rivera*, K.D.P. Nigam******

**Chemical Engineering Department, Universidad Michoacana de San Nicolas de Hidalgo, Morelia, Michoacan, 58060, Mexico (e-mail: ilsehdz_07utlook.com)*

***Tecnologico de Monterrey, Escuela de Ingeniería y Ciencias, Ave. Eugenio Garza Sada 2501, Monterrey, N.L., 64849, Mexico. (e-mail: antonio.flores.t@tec.mx)*

**** Department of Chemical Engineering, Tecnológico Nacional de México en Celaya, Celaya Gto. 38010, Mexico*

***** Department of Chemical Engineering, Indian Institute of Technology, Delhi −110016, India*

Abstract: The heat conduction in steady state is one of the problems of analysis commonest in the study of the diverse associated physical phenomena to heat transference in many processes. In this work, the two-dimensional heat conduction of rectangular coordinates on a square plate is analyzed. The system under consideration is a mixture of metallic nano-sized particles and conventional heat-transferring fluid. In this sense, a mathematical optimization model is proposed to get the optimal distribution of the nanoparticles within the base fluid allowing minimizing the resistance to heat transfer in the system as an objective function and with this improving the thermal performance of the nanofluid. Considering that the nanofluids performance counts on nanoparticle configuration. In addition, Neumann and Dirichlet boundary conditions are considered as restrictions of the problem. For the numerical formulation, the finite difference method in Matlab® is used.

Keywords: Nonlinear equations, Partial differential equations, Conductivity, Boundary Conditions, Heat conduction

https://doi.org/10.1016/j.ifacol.2019.08.03

Hernández-Romero, I. M., Flores-Tlacuahuac, A., Fuentes-Cortés, L. F., Nápoles-Rivera, F., & Nigam, K. D. P. (2019). Optimal configuration of metallic nanoparticles to maximize heat transfer in a 2D square plate. IFAC-PapersOnLine, 52(2), 207-211.

Chemical Engineering & Processing: Process Intensification 157 (2020) 108114

Contents lists available at ScienceDirect

Chemical Engineering and Processing - Process Intensification

journal homepage: www.elsevier.com/locate/cep

Optimal design of the ocean thermal energy conversion systems involving weather and energy demand variations

Ilse María Hernández-Romero [a], Fabricio Nápoles-Rivera [a], Antonio Flores-Tlacuahuac [b], Luis Fabián Fuentes-Cortés [c,*]

[a] Chemical Engineering Department, Universidad Michoacana de San Nicolás de Hidalgo, Morelia, Michoacán, 58060, Mexico
[b] Tecnologico de Monterrey, Escuela de Ingeniería y Ciencias, Ave. Eugenio Garza Sada 2501, Monterrey, N.L., 64849, Mexico
[c] Tecnológico Nacional de México - Instituto Tecnológico de Celaya, Departamento de Ingeniería Química, Celaya Guanajuato, 38010, Mexico

ARTICLE INFO

Keywords:
Ocean thermal energy conversion systems
Multi-objective optimization
Closed power cycle
Exergy analysis
Multi-period operation

ABSTRACT

Ocean thermal energy conversion systems (OTEC) represent an attractive economic alternative in communities allocated in coastal areas for producing electric utilities reducing fossil fuel consumption and emissions. This power generation technology uses the temperature difference between the deep cold water and warm surface water of the ocean to produce electricity using the principles of the Rankine cycle. This paper presents a Non-Linear Programming (NLP) multi-period and multi-objective model for the analysis of OTEC systems. The multi-objective approach consists in to maximize the exergy efficiency of the cycle while the total annual cost of the system is minimized. Variations on solar resources availability, energy demands, and ambient conditions are addressed considering hourly and seasonal profiles from a given housing complex allocated on the Pacific Coast from Mexico.

https://doi.org/10.1016/j.cep.2020.108114

Highlights

- Optimal design of oceanic thermal energy conversion systems is addressed.
- The model considers variations in energy demand and ambient conditions.
- The proposed model presents a Multi-period and multi-scenario approach.
- Multi-objective NLP model considers total annual cost and exergy performance.
- Utopia tracking approach is used for reaching a trade-off solution.

Hernández-Romero, I. M., Nápoles-Rivera, F., Flores-Tlacuahuac, A., & Fuentes-Cortés, L. F. (2020). Optimal design of the ocean thermal energy conversion systems involving weather and energy demand variations. *Chemical Engineering and Processing-Process Intensification*, *157*, 108114.

Contents lists available at ScienceDirect

Computers and Chemical Engineering

journal homepage: www.elsevier.com/locate/compchemeng

A MINLP approach to improve heat transfer in flat plates through the optimal distribution of nanoparticles

Ilse María Hernández-Romero[a], Antonio Flores-Tlacuahuac[d,*], Luis Fabián Fuentes-Cortés[c], Fabricio Nápoles-Rivera[a], K.D.P. Nigam[b,d]

[a] Chemical Engineering Department, Universidad Michoacana de San Nicolas de Hidalgo, Morelia, Michoacan 58060, Mexico
[b] Department of Chemical Engineering, Indian Institute of Technology, Delhi 110016, India
[c] Tecnologico Nacional de Mexico - Instituto Tecnologico de Celaya, Departamento de Ingeniería Química, Celaya, Gto. 38010, Mexico
[d] Tecnologico de Monterrey, Escuela de Ingeniería y Ciencias, Ave. Eugenio Garza Sada 2501, Monterrey, N.L. 64849, Mexico

ARTICLE INFO

Article history:
Received 6 September 2020
Revised 21 May 2021
Accepted 28 May 2021
Available online 17 June 2021

Keywords:
Heat transfer
Steady state
Heat conduction
Partial differential equations (PDE)
Nanofluids
MINLP optimization

ABSTRACT

In this work, the thermal effect of deploying nanoparticles on the steady-state two-dimensional heat transfer behavior on a square plate is presented. The aim is to strengthen process intensification through efficient energy use. The approach of this work is to present a general methodology to obtain the optimal configuration of the nanoparticles and the base fluid respectively in the system. Here, the objective function is maximizing the heat transfer of the system considering that the performance of the nanofluids depends on the distribution of the nanoparticles. A general model is presented that allows solving the two-dimensional heat equation for the nanoparticles and the base fluid independently. The mathematical formulation is presented as a problem of Mixed-Integer Non-linear Programming (MINLP) model. The system under consideration is a mixture of metallic nano-sized particles and conventional heat-transferring fluid. In addition, it is also considered that there is heat generation inside the base fluid and as well the thermal conductivity of the flat plate is assumed to vary as a linear function of the temperature. The results indicate that improved heat transfer can be achieved through optimal fluid location. However, in few cases this behavior was not observed and the explanation of this issue is linked to the the nonconvex MINLP problem rendering only optimal local solutions. In order to show the applicability of the proposed methodology, two parametric case studies are presented.

https://doi.org/10.1016/j.compchemeng.2021.107389

Highlights

A novel MINLP optimization formulation is proposed for the optimal location of nanofluids in energy systems.

- The optimization formulation can help to enhance energy efficiency in heat transfer equipment.
- A steady-state 2 dimensional partial differential equation model was considered for modeling purposes.
- Random location of nanofluids was not able to outperform MINLP optimal results.

Hernández-Romero, I. M., Flores-Tlacuahuac, A., Fuentes-Cortés, L. F., Nápoles-Rivera, F., & Nigam, K. D. P. (2021). *A MINLP approach to improve heat transfer in flat plates through the optimal distribution of nanoparticles*. Computers & Chemical Engineering, 152, 107389.